ATM Is Required for the Prolactin-Induced HSP90-Mediated Increase in Cellular Viability and Clonogenic Growth After DNA Damage

Ödül Karayazi Atici,[1,2] Anna Urbanska,[1,2] Sesha Gopal Gopinathan,[1,2] Florence Boutillon,[3] Vincent Goffin,[3] and Carrie S. Shemanko[1,2]

[1]Department of Biological Sciences, University of Calgary, Calgary, Alberta T2N 1N4, Canada; [2]Arnie Charbonneau Cancer Institute, University of Calgary, Calgary, Alberta T2N 1N4, Canada; and [3]Inserm U1151, Institut Necker Enfants Malades, Team "PRL/GH Pathophysiology," Faculty of Medicine Paris Descartes, Sorbonne Paris Cité, 75993 Paris cedex 14, France

Prolactin (PRL) acts as a survival factor for breast cancer cells, but the PRL signaling pathway and the mechanism are unknown. Previously, we identified the master chaperone, heat shock protein 90 (HSP90) α, as a prolactin–Janus kinase 2 (JAK2)–signal transducer and activator of transcription 5 (STAT5) target gene involved in survival, and here we investigated the role of HSP90 in the mechanism of PRL-induced viability in response to DNA damage. The ataxia–telangiectasia mutated kinase (ATM) protein plays a critical role in the cellular response to double-strand DNA damage. We observed that PRL increased viability of breast cancer cells treated with doxorubicin or etoposide. The increase in cellular resistance is specific to the PRL receptor, because the PRL receptor antagonist, Δ1-9-G129R-hPRL, prevented the increase in viability. Two different HSP90 inhibitors, 17-allylamino-17-demethoxygeldanamycin and BIIB021, reduced the PRL-mediated increase in cell viability of doxorubicin-treated cells and led to a decrease in JAK2, ATM, and phosphorylated ATM protein levels. Inhibitors of JAK2 (G6) and ATM (KU55933) abolished the PRL-mediated increase in cell viability of DNA-damaged cells, supporting the involvement of each, as well as the crosstalk of ATM with the PRL pathway in the context of DNA damage. Drug synergism was detected between the ATM inhibitor (KU55933) and doxorubicin and between the HSP90 inhibitor (BIIB021) and doxorubicin. Short interfering RNA directed against ATM prevented the PRL-mediated increase in cell survival in two-dimensional cell culture, three-dimensional collagen gel cultures, and clonogenic cell survival, after doxorubicin treatment. Our results indicate that ATM contributes to the PRL–JAK2–STAT5–HSP90 pathway in mediating cellular resistance to DNA-damaging agents. (***Endocrinology*** **159: 907–930, 2018)**

Prolactin (PRL) is an essential mediator of mammary gland development, stimulating the mammary alveolar cell proliferation and differentiation during pregnancy and lactation (1); however, it also plays an important role in the pathogenesis and progression of breast cancer (2) and breast cancer bone metastases (3, 4)

ISSN Online 1945-7170

Received 19 July 2017. Accepted 21 November 2017.
First Published Online 24 November 2017

Abbreviations: 2D, two-dimensional; 3D, three-dimensional; 17-AAG, 17-allylamino-17-demethoxygeldanamycin; ANOVA, analysis of variance; ATM, ataxia–telangiectasia mutated kinase; BRCA1, breast cancer-1; BSA, bovine serum albumin; cDNA, complementary DNA; CI, combination index; DMSO, dimethyl sulfoxide; ECL, enhanced chemiluminescence; ER, estrogen receptor; GRB2, growth factor receptor–bound protein 2; hPRL, human prolactin; HRP, horseradish peroxidase; HSP90, heat shock protein 90; JAK2, Janus kinase 2; MRN, Mre11-Rad50-Nbs1; mRNA, messenger RNA; oPRL, ovine prolactin.; *p*-ATM, phosphorylated ataxia–telangiectasia mutated kinase; PBS, phosphate-buffered saline; PPARγ, peroxisome proliferator–activated receptor γ; PRL, prolactin; PRLR, prolactin receptor; *p*-STAT5, phosphorylated signal transducer and activator of transcription 5; qPCR, quantitative polymerase chain reaction; SDS-PAGE, sodium dodecyl sulfate–polyacrylamide gel electrophoresis; siATM, short interfering RNA directed against ataxia–telangiectasia mutated kinase; siNT, nontargeting short interfering RNA; siRNA, short interfering RNA; STAT5, signal transducer and activator of transcription 5; TBST, Tris-buffered saline and polysorbate 20; TEL2, telomere maintenance-2; w/v, weight-to-volume ratio; YWHAZ, tyrosine 3-monooxygenase/tryptophan 5-monooxygenase activation protein ζ.

including possible resistance to cytotoxic drugs (5, 6). There is much that we do not understand about the contribution of PRL and the PRL receptor (PRLR), as there is a spectrum of reports regarding their role. Epidemiological studies have shown that increased circulating PRL levels are positively correlated with increased breast cancer risk, disease recurrence, and poor outcome (7–9). The role of PRL in mouse mammary cancer initiation (10, 11) and human breast cancer progression (7, 12) has become increasingly recognized as a contributor to the disease. However, some retrospective studies of PRLR gene expression have been associated with a favorable prognosis (13, 14). This finding contrasts with functional studies that indicate the PRLR functions in human breast epithelial cell transformation (15) and metastasis (16). There are multiple PRLR isoforms, created by alternative splicing, that display different signal transduction capacities in the cytoplasm (17–20); their specific functions have not been fully elucidated (2). It has been demonstrated that autocrine PRL is also produced in human breast tumors (21). PRL promotes cell survival (21–25) and is associated with poor relapse-free survival and overall survival (26). Autocrine PRL may explain why decades ago inhibitors of PRL secretion from the pituitary gland were not completely successful treatments for advanced breast cancer (27, 28). PRLR expression is reported with both estrogen receptor (ER) positive and ER negative breast tumors (4, 29–31), the latter of which are associated with poor prognosis.

The role of PRL in cytotoxic resistance in breast cancer cells treated with vinblastine, taxol, cisplatin (32), paclitaxel (33), and doxorubicin (32, 33) has been reported *in vitro*. High serum PRL levels were also found in patients with metastatic breast cancer in association with resistance to taxanes (6). PRL contributes to *in vitro* cell survival after chemotherapeutic drug treatment, although the downstream mechanisms are not well understood.

We previously identified the master cancer chaperone heat shock protein 90α (HSP90α) as a PRL–Janus kinase 2 (JAK2)–signal transducer and activator of transcription (STAT) 5b regulated gene in breast cancer cells (30). We observed that PRL and HSP90α promoted cellular survival of normal mammary epithelial cells and breast cancer cells in a cellular context-dependent manner. We discovered that immortal HC11 cells were more sensitive than breast cancer SKBR3 cells to apoptotic induction when both were overexpressing HSP90α.

The more inducible HSP90α and the more constitutive HSP90β are produced from two distinct genes with high homology and have some reported differential functions but are collectively known as HSP90, the master cancer chaperone (34, 35). HSP90 expression is elevated in breast cancers and correlated with decreased patient survival (36–38). HSP90α is associated with cellular transformation (39) and invasion (40). HSP90α clients are involved in pathways responsible for cancer cell survival, cell cycle control, and DNA repair, and inhibitors of HSP90 (HSP90α and HSP90β), such as 17-allylamino-17-demethoxygeldanamycin (17-AAG) (tanespimycin), have been used in clinical trials for breast and other cancers (35, 41–46). The inhibitor BIIB021 is a synthetic nonansamycin HSP90 inhibitor also in clinical development and has the advantage of being able to be administered orally (47). These clinically tested inhibitors interact with the adenosine triphosphate binding pocket of HSP90, resulting in destabilization and degradation of virtually all client proteins (41, 45, 46). HSP90 inhibitors bind specifically and preferentially to HSP90 proteins in cancerous cells rather than normal cells (48) and preferentially in tumor-initiating cells (49).

Recent studies have shown that the activation and stability of JAK2 depend on HSP90 and that JAK2 is a *bona fide* client protein of HSP90 chaperone complex in leukemia cells (50, 51). It is known that HSP90 client proteins (*i.e.*, substrates of HSP90) depend on HSP90 for maturation or stability, and inhibition of HSP90 will result in their loss due to proteolytic degradation (45).

HSP90 is intricately involved in the DNA damage response by chaperoning key proteins of different response and repair pathways, including XRCC1 (52), breast cancer-1 (BRCA1) (53), checkpoint kinase-1 (54), ataxia telangiectasia– and RAD3-related protein (ATR) (55), and the Mre11-Rad50-Nbs1 (MRN) complex (56). Ataxia–telangiectasia mutated kinase (ATM) and other family members such as ATR and DNA-dependent protein kinase catalytic subunit (57) are sensitive to HSP90 inhibition (58) indirectly via its interaction with telomere maintenance-2 (TEL2) (58, 59), which forms a scaffold for HSP90 chaperone interaction (57). Inhibition of HSP90 results in degradation of the DNA damage response proteins, which leads to deficits in DNA repair. HSP90 was shown to be essential for ATM to become a functionally mature protein (58, 60), although at maturity the cochaperone complex was no longer needed (58).

ATM is a central mediator (61) in response to 10% to 20% of the cell's double-strand DNA breaks (62), particularly those in heterochromatin (63) or those with blocked ends (64). Blocked double-strand breaks arise naturally or in the presence of topoisomerase II poisons, such as etoposide and doxorubicin, which result in stabilized intermediate complexes created by topoisomerase activity. Topoisomerase activity is necessary to relieve the topological constraints created during replication or transcription, by creating a controlled double-strand

break (65). The intermediate complexes created by topoisomerase II poisons contain topoisomerase II covalently bonded to the cleaved ends of the DNA, which would normally be quickly resolved. The stabilized intermediate contains peptidic DNA ends that equate to the blocked ends of the double-strand break. This ATM-based repair pathway of these blocked ends is important for cell survival and genomic stability (64).

In light of previous studies that indicate PRL contributes *in vitro* to increased survival in the presence of DNA-damaging agents, we aimed to test the hypothesis that PRL signaling interacts with the DNA damage response in an HSP90-mediated manner. As described below, our observations identify a HSP90-based mechanism by which PRL and ATM increase cell viability and clonal growth despite DNA-damaging anticancer agents.

Materials and Methods

Materials

Recombinant human PRL (hPRL) and the PRLR antagonist Δ1-9-G129R-hPRL were produced and chromatography-purified as previously described (66). Ovine prolactin (oPRL), doxorubicin, etoposide, and 17-AAG were purchased from Sigma-Aldrich (Oakville, ON, Canada). KU55933 (Tocris, Minneapolis, MN), G6 (NSC33994), and BIIB021 (Selleck Chemicals, Houston, TX) were resuspended in appropriate amounts of dimethyl sulfoxide (DMSO).

Antibodies

We used the following antibodies: monoclonal anti-extracellular PRLR domain (1A2B1; Thermo Fisher Scientific, Wilmington, DE; AB_2533231), rabbit monoclonal anti-phosphorylated STAT5 pY694 (E208; Abcam, Toronto, ON, Canada; AB_778105), rabbit anti-STAT5 (Cell Signaling Technologies, Beverly, MA; catalog no. 9363S; AB_10693321) or mouse anti-STAT5 (BD Biosciences, Mississauga, ON, Canada; catalog no. 61092; AB_397591), rabbit anti-histone H3 (Millipore, Etobicoke, ON, Canada; AB_991678), rabbit anti-phosphorylated-ATM-protein kinase pS1981 (Epitomics; clone EP1890Y; Cedarlane, Burlington, ON, Canada; AB_368161), mouse anti-ATM monoclonal antibody (clone 2C1; Gene Tex, San Antonio, TX; AB_368161), rabbit anti-HSP90α (catalog no. SPS-771; StressGen, Victoria, BC, Canada; AB_1534201), mouse anti–growth factor receptor–bound protein 2 (GRB2) (clone 81/GRB2; BD Biosciences; AB_397517), anti-JAK2 D2E12 rabbit monoclonal antibody (Cell Signaling Technologies; catalog no. 3230; AB_2128522), horseradish peroxidase (HRP)–conjugated goat anti-rabbit (Bio-Rad, Mississauga, ON, Canada), and HRP-conjugated goat anti-mouse secondary antibody (Bio-Rad).

Cell culture and cell lines

PRL-responsive SKBR3 (HER2 overexpressing, p53 mutant) and MCF7 (estrogen receptor+, p53 wild type) human breast cancer cell lines, obtained and authenticated from American Type Culture Collection, were used within 6 months when revived from frozen storage. They were maintained in Dulbecco's modified Eagle medium (Invitrogen, Burlington, ON, Canada) and supplemented with 10% fetal bovine serum (PAA Laboratories Inc., Etobicoke, ON, Canada), 100 μg/mL streptomycin and 100 U/mL penicillin, 2 mM L-glutamine (Invitrogen), and, for MCF7, also 10 μg/mL insulin (BD Biosciences). L3 cells were a gift from Dr. Susan Lees-Miller (University of Calgary).

Slope and intercept experiments

Cells were plated at 5000 cells per well of a 96-well plate for 24 hours, followed by treatment or vehicle with doxorubicin for 2 hours with 48 hours of recovery. Cells were counted with trypan blue exclusion or WST-1 assay. The percentage cell survival from WST-1 assay was entered into GraphPad Software (GraphPad Software, San Diego, CA), best-fit values of slope and intercept were calculated with a linear regression model, and *P* values were calculated from the *F* test.

WST-1 cell proliferation assay

Cells were seeded at 5000 cells per well into 96-well cell culture plates for 12 hours, before pretreatments of PRL or inhibitor (17-AAG, BIIB021, Ku55933) for 24 hours (or 12 hours for G6) followed by 2 hours doxorubicin treatment with or without PRL or inhibitor as indicated. Doxorubicin was removed and cells recovered for 48 hours with or without PRL or inhibitor. Control cells were treated with appropriate amounts of vehicle, phosphate-buffered saline (PBS), or DMSO. WST-1 reagent (Roche, Laval, QC, Canada) was added to each well according to the manufacturer. The surviving fraction was calculated from pooled experiments and surviving cells presented as a percentage of the untreated vehicle controls that were set to 100%.

Inhibition of PRL signaling

SKBR3 breast cancer cells (1×10^6) were plated into 10-cm cell cultures dishes 2 days before the experiment. After 24 hours of cell culture, cells were subjected to starvation in serum-free medium for a maximum of 16 hours. Immediately after starvation, cells were treated with oPRL (5 μg/mL) or Δ1-9-G129R-hPRL (5 μg/mL) for 1 hour or left untreated.

Whole cell lysate extract with NP-40 buffer

To prepare cell extracts to detect phosphorylated ATM (*p*-ATM), ATM, HSP90, and GRB2, SKBR3 or MCF7 cells were washed twice with 1× PBS and scraped into 1.5-mL microcentrifuge tubes. After centrifugation at 12,000 rpm for 10 minutes at 4°C (Eppendorf 5415R microcentrifuge), the supernatant was removed. The pellet was resuspended in 1% NP-40 lysis buffer containing 1% Nonidet-P-40, 50 mM Tris-HCl pH 7.5, 5 mM EGTA, and 200 mM NaCl. Protease and phosphatase inhibitors were freshly added as follows: 1 mM sodium vanadate (Sigma-Aldrich), 20 nM phenylarsine oxide (EMD Millipore), 1 μg/mL leupeptin (EMD Millipore), 0.5 μg/mL aprotinin (Sigma-Aldrich), 100 μM phenylmethylsulfonyl fluoride (Sigma-Aldrich), 1 μM dithiothretiol (Fermentas), and 1 μg/mL pepstatin (Sigma-Aldrich). The extracts were incubated for 20 minutes at 4°C followed by centrifugation at 12,000 rpm for 10 minutes at 4°C. The supernatant was snap frozen.

Protein extraction and sodium dodecyl sulfate polyacrylamide gel electrophoresis

Extracts for the detection of the PRLR were prepared with Complete Lysis M Buffer (Roche) and protease inhibitors (Roche; catalog no. 04719956001), as per the manufacturer's protocols.

To prepare whole cell extracts to detect JAK2, cells were washed twice with PBS and scraped in sample buffer containing 2% [weight-to-volume ratio (w/v)] sodium dodecyl sulfate, 10% (w/v) glycerol, 100 mM dithiothretiol, 0.02% (w/v) bromophenol blue, 1 M Tris-HCl pH 6.8, followed by sonication three times for 5 seconds with a 5-second interval (Fisher Scientific 60 Sonic Dismembrator) on ice. Protein concentration was determined, and proteins were snap frozen.

Nuclear proteins (67) were resolved on a triple gel system with one layer of 15% acrylamide resolving gel at the bottom, one layer of 8% acrylamide resolving gel, and one layer of 5% acrylamide stacking gel (30).

Western blot analysis

To detect phosphorylated STAT5 (*p*-STAT5), the membrane was incubated overnight at 4°C with a rabbit monoclonal antibody against pY694, diluted 1:1000 in 5% bovine serum albumin (BSA) in 0.05% Tris-buffered saline and polysorbate 20 (TBST). Alternatively, *p*-STAT5 was detected with HRP-conjugated goat anti-rabbit secondary antibody and enhanced chemiluminescence (ECL) (30). The membrane was stripped (100 mM 2-mercaptoethanol, 2% sodium dodecyl sulfate, 62.5 mM Tris-HCl pH 6.8) at 60°C for 30 minutes with gentle agitation, then washed with 0.05% TBST. To detect STAT5, the membrane was incubated overnight at 4°C in mouse anti-STAT5 antibody diluted 1:1000 in 5% BSA in TBST 0.05% and detected with HRP-conjugated goat anti-mouse secondary antibody and ECL (30).

To detect *p*-ATM, the membrane was incubated overnight at 4°C with rabbit anti-ATM protein kinase pS1981, diluted 1:5000 in 0.1% gelatin in 0.1% TBST. The next day *p*-ATM was detected with HRP-conjugated goat anti-rabbit secondary antibody and ECL. To detect ATM, the stripped membrane was incubated overnight at 4°C in mouse anti-ATM monoclonal antibody diluted 1:3000 in 1% BSA in TBST 0.1% and detected with HRP-conjugated goat anti-mouse secondary antibody and ECL.

To detect HSP90α, the membrane was incubated overnight at 4°C with rabbit anti-HSP90α diluted 1:5000 in 15% BSA in 0.05% TBST.

To detect GRB2, the membrane was incubated overnight at 4°C with mouse anti-GRB2, diluted 1:5000 in 3% BSA in 0.05% TBST before detection with an HRP-conjugated goat anti-mouse secondary antibody and ECL.

JAK2 and the PRLR (1:1000) were detected according to manufacturers' protocols.

Quantification of Western blots

ImageJ software was used to quantify the signal intensity on the Western blot images (68). Alternatively, the Amersham Imager 600 (GE Healthcare Life Sciences) was used.

Knockdown with short interfering RNA

All knockdown experiments were performed with ON-TARGET*plus* ATM SMARTpool short interfering RNA (siRNA) (5 nmol) [short interfering RNA directed against ataxia–telangiectasia mutated kinase (siATM)] (69) or ON-TARGET*plus* Nontargeting Pool (universal negative control; Dharmacon D-001810-10-05) siRNA (5 nmol) [nontargeting short interfering RNA (siNT)] and DharmaFect transfection reagent from GE Healthcare (Lafayette, CO). Manufacturer's instructions were followed for knockdown experiments and percentage knockdown calculations. The expression of the target gene (ATM) was first normalized to the reference gene tyrosine 3-monooxygenase/tryptophan 5-monooxygenase activation protein ζ (YWHAZ) expression before normalizing expression to the siNT.

Clonogenic cell survival assay with siRNA transfected cells

MCF7 or SKBR3 cells (5000 cells) were plated into 96-well plates and the next day transfected with ATM or siNT. After 48 hours of transfection, cells were pretreated with recombinant hPRL (25 ng/mL) or PBS for 24 hours followed by 2 hours of doxorubicin treatment with or without PRL. After doxorubicin treatment, cells were transferred to 6-well plates. The cells were stained with 0.5% gentian violet after 10 days of growth. Colonies of >30 cells (SKBR3) or >50 cells (MCF7), were counted under the light microscope.

RNA extraction and complementary DNA synthesis

RNA was extracted from breast cancer cells with a Qiagen RNEasy Mini Kit (Qiagen Inc., Missisauga, ON, Canada) according to supplied protocols.

Complementary DNA (cDNA) was synthesized from 2 μg of RNA with a SuperScript II reverse transcription kit (Invitrogen) according to the manufacturer's protocol.

Quantitative polymerase chain reaction

All primers were designed with the NCBI Primer-BLAST program. Operon's Oligo Analysis Tool was used to detect possible primer dimmers, and self-complementation was identified with IDT's OligoAnalyzer. The desired primers were obtained from University of Calgary DNA Synthesis Laboratory (Calgary, AB, Canada).

Quantitative polymerase chain reactions (qPCRs) were carried out with iTaq Universal SYBR Green Supermix (Bio-Rad) with 1 μL each of forward and reverse primer (final primer concentration of 10 μM) and 1 μL cDNA and brought up to 20 μL with double-distilled H_2O. Each reaction was performed in triplicate, pipetted into 96-well polymerase chain reaction plates (Bio-Rad), and sealed with optical sealing tape (Bio-Rad). Reactions were cycled on the Bio-Rad iQ5 Real-Time PCR Detection System (University of Calgary).

Primer sequences for ATM were as follows: forward primer 5′-CTGTGCAGCGAACAATCCCA-3′ and reverse primer 5′-TAACCAGTTGCCACAAACCCT-3′, with an expected amplicon of 70 base pairs. ATM amplification was performed according to the following protocol: 95°C for 2 minutes, 40 cycles of 95°C for 10 seconds, 58°C for 30 seconds, 78°C for 20 seconds, and a final extension step of 72°C for 10 minutes.

Primer sequences for JAK2 were designed as follows: forward primer 5′-TACCTCTTTGCTCAGTGGCG-3′ and reverse primer 5′-ACTGCCATCCCAAGACATTC-3′, with an expected amplicon of 95 base pairs. JAK2 amplification was performed according to the following protocol: 95°C for

2 minutes, 40 cycles of 95°C for 10 seconds, 58°C for 30 seconds, 78°C for 20 seconds, and a final extension step of 72°C for 10 minutes.

YWHAZ primer sequences are as follows: forward primer 5′-AGTCGTACAAAGACAGCACGTAA-3′ and reverse primer 5′-AGGCAGACAAAGGTTGGAAGG-3′, with an expected amplicon of 138 base pairs. The following protocol was used for amplification of the YWHAZ gene: 95°C for 2 minutes, 40 cycles of 95°C for 10 seconds, 60°C for 30 seconds, 78°C for 20 seconds, and final extension step of 72°C for 10 minutes.

Combination index

MCF7 cells were plated into 96-well cell culture plates. Cells were pretreated with KU55933 or BIIB021 for 24 hours, followed by 2 hours of doxorubicin treatment in the presence of inhibitors. Fixed concentrations of BIIB021 (400 nM and 800 nM) and KU55933 (10 μM and 20 μM) were used with threefold increasing concentrations of doxorubicin during drug combination treatments. All drugs were removed from the media except KU55933 during the 48-hour recovery time. Cell viability was assessed with the WST-1 cell viability assay. All treatments were normalized to vehicle controls.

The cell viability results from drug treatments alone and in combination were entered into the CompuSyn program (ComboSyn, Inc.) of Chou (70) to evaluate the synergism, additive effect, or antagonism between combined drugs. The computer program used Chou median-effect equation, which is described as "fa/fu = D/Dm" (fa = affected cell fraction, fu = unaffected cell fraction, D = dose of the drug, Dm = median effect dose, m = slope of the median effect curve) (70). The combination index (CI) calculated from the equation indicates synergism if CI $<$ 1, additive effect if CI = 1, and antagonism if CI $>$ 1. According to the detailed description, a CI value $<$0.1 indicates very strong synergism, a CI value between 0.1 and 0.3 indicates strong synergism, a CI value between 0.3 and 0.7 indicates synergism, a CI value between 0.7 and 0.85 indicates moderate synergism, a CI value between 0.85 and 0.90 indicates slight synergism, and a CI value between 0.9 and 1.1 indicates nearly additive effect.

Collagen three-dimensional cell viability assay

SKBR3 and MCF7 (4.5×10^5) cells were plated into 6-cm dishes for 24 hours, before pretreatment of 25 ng/mL hPRL for 24 hours, followed by 2 hours of doxorubicin treatment (1 μM) or vehicle with hPRL or vehicle. Doxorubicin was removed and 5000 cells were transferred to three-dimensional (3D) culture of 2.8 mg/mL type I rat tail collagen (Corning, VWR, Mississauga, ON, Canada) in 96-well plates, prepared as per the manufacturer's instructions, in the presence of 25 ng/mL hPRL or vehicle. The cells recovered for 48 hours with PRL or vehicle in high-density collagen. Control cells were treated with appropriate amounts of PBS or DMSO. WST-1 reagent was added to each well according to the manufacturer. The surviving fraction was calculated by normalization to the control conditions and expressing surviving cells as a percentage of the untreated controls set to 100%.

Collagen 3D cell viability assay with siRNA transfected cells

MCF7 or SKBR3 cells, were plated at 2.5×10^5 cells per well into six-well plates and next day transfected with siATM or siNT as described above. After 48 hours of transfection, cells were pretreated with hPRL (25 ng/mL) for 24 hours, followed by 2 hours of doxorubicin (2 μM for MCF7 cells, 3 μM for SKBR3 cells) treatment with hPRL or vehicle. After doxorubicin treatment, cells were transferred to 3D collagen gels in 96-well plates, and viability was assayed by WST-1 assay after 48 or 96 hours, as described above.

Statistical analysis

Statistical significance was tested with a paired Student *t* test with a two-tailed distribution and considered significant at $P < 0.05$. Alternatively, a one-way analysis of variance (ANOVA) was used with posttesting, and results were considered significant at $P < 0.05$.

Results

PRL increases the resistance of breast cancer cells to DNA-damaging agents

To introduce DNA damage, we used the topoisomerase II poisons doxorubicin and etoposide (71), which result primarily in double-strand DNA breaks (72) and single-strand breaks (73), respectively, and produce blocked double-strand lesions (64). Despite the predominance of single-strand breaks, it is believed that etoposide-induced toxicity is due to the double-strand breaks (73). We treated two PRL-responsive breast cancer cell lines (SKBR3 and MCF7) with a range of doxorubicin and etoposide concentrations known to induce DNA damage and investigated ATM phosphorylation at serine-1981, which is indicative of the double-strand DNA damage response (74). SKBR3 (Fig. 1A and 1C) and MCF7 (Fig. 1B and 1D) were treated with increasing doses of doxorubicin or etoposide. Increasing amounts of *p*-ATM were detected across the dose ranges, indicating that both cell lines responded to the DNA damage induced by the topoisomerase II poisons.

We next assessed cell viability by using the WST-1 assay. The WST-1 assay has been used to measure cell viability after treatment with toxic compounds, such as chemotherapeutics, including the HSP90 inhibitor 17-AAG, in cell lines such as MCF7 (75). As a control to compare any differences between this mitochondrial cell viability assay and the number of surviving cells, based here on trypan blue exclusion, MCF7 and SKBR3 cells were treated with doxorubicin, and the cell viability was measured with the WST-1 assay or viable cells were counted under light microscopy after 48 hours. There was no difference between the slopes of each assay for SKBR3 (Fig. 2A) or MCF7 cells (Fig. 2B). The difference in percentage survival of the control illustrates that the WST-1 viability assay is sensitive to cell death induced by doxorubicin and allows a consistent and high-throughput analysis.

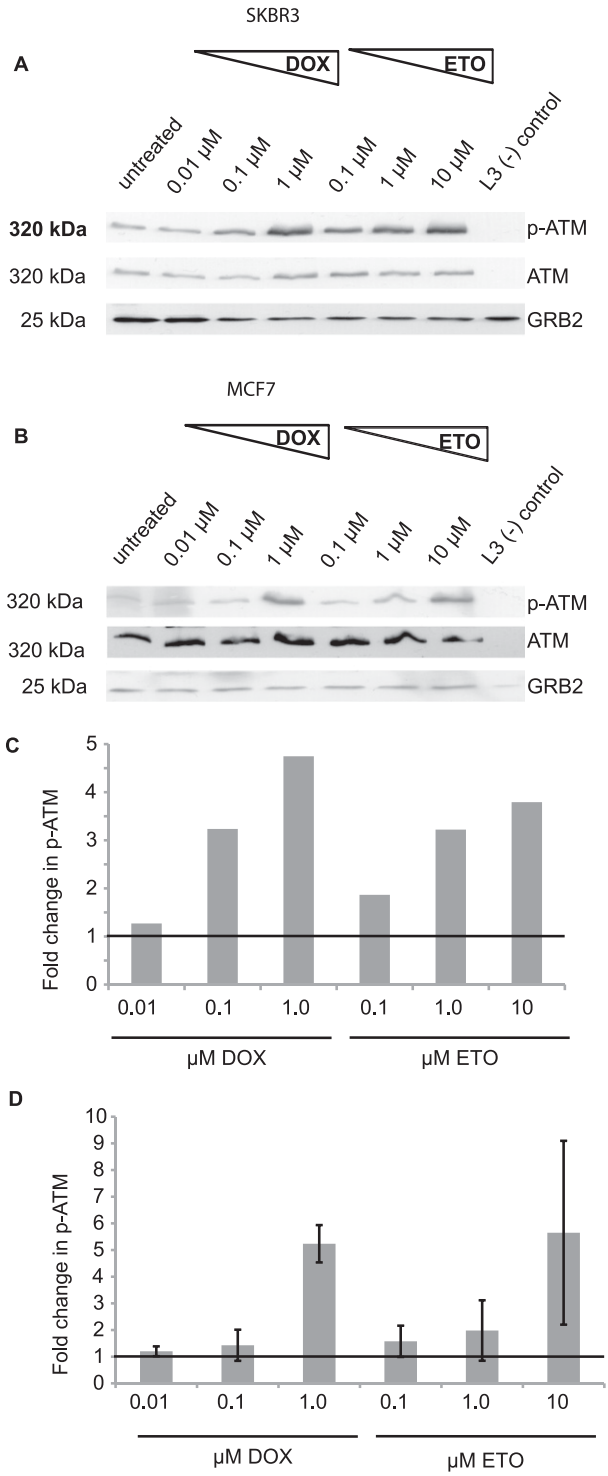

Figure 1. ATM is activated in SKBR3 and MCF7 cells in response to doxorubicin (DOX) and etoposide (ETO) treatment. (A) SKBR3 or (B) MCF7 cells were treated for 2 hours with DOX or ETO followed by protein extraction and Western blot. Proteins (20 μg/lane) were resolved on sodium dodecyl sulfate–polyacrylamide gel electrophoresis gel and blot was probed for *p*-ATM, total ATM, and GRB2. (C and D) ImageJ quantification of fold change of *p*-ATM compared with untreated (*p*-ATM normalized to ATM levels) in (C) SKBR3 and (D) MCF7 cells (error bars show standard deviation of two independent experiments pooled). Untreated samples were set to a fold change of 1 and indicated as a solid horizontal line. L3 ATM null cells were used as a negative control for ATM.

To determine whether PRL could increase the viability of cells treated with DNA-damaging agents, as previously observed with doxorubicin (32, 33), we pretreated the cells with or without PRL before introducing DNA damage and maintained the cells in the presence or absence of PRL throughout the experiment as per the initial treatment. We first tested oPRL, which increased cell viability across all concentrations of doxorubicin. oPRL increased cell viability in doxorubicin-treated SKBR3 cells by ≤9% (Fig. 2C) and in doxorubicin-treated MCF7 cells, by ≤13% (Fig. 2D) compared with doxorubicin treatment alone. Because oPRL is prepared from a pituitary source and may contain additional hormones, we aimed to confirm these findings with a pure preparation of recombinant hPRL. Human PRL receptors are 10 times more sensitive to hPRL than to oPRL (76). We used a dose of hPRL, 25 ng/mL, that is representative of high-normal serum levels associated with elevated breast cancer risk (77–79). Human PRL was also able to increase the viability of doxorubicin-treated SKBR3 cells by ≤14% (Fig. 2E) and in doxorubicin-treated MCF7 cells ≤12% (Fig. 2F). Overall, the MCF7 cell line was more resistant to doxorubicin than the SKBR3 cell line. Both oPRL and hPRL increased the viability of breast cancer cells treated with doxorubicin, consistent with levels previously reported (32, 33).

We additionally treated breast cancer cells with single doses of etoposide and investigated their response to oPRL. Based on dose-response studies (80), we chose a concentration of etoposide that would reduce viability to ~80% for each cell line. SKBR3 cells were again more sensitive to etoposide than MCF7 cells. PRL treatment resulted in increased cell viability by ≤18% in SKBR3 cells (Fig. 2G) and by ≤15% in MCF7 cells (Fig. 2H) treated with 2 μM or 10 μM etoposide, respectively. Together these data support our hypothesis that PRL increases the viability of breast cancer cells treated with DNA-damaging topoisomerase II poisons.

DNA damage resistance is mediated by the PRLR

To determine that the PRL-induced resistance to topoisomerase II poisons was specific to the PRLR, we used the pure PRLR antagonist Δ1-9-G129R-hPRL (66). Both SKBR3 and MCF7 cells have similar amounts of the long full-length and short 1b PRLR isoforms, but SKBR3 cells contain greater levels of the intermediate isoform (Fig. 3A). We first assessed the phosphorylation of STAT5 as a readout of the PRL-JAK2-STAT5 pathway (81). Given the 10-fold lower sensitivity of the human PRLR to oPRL (76), the equimolar concentration of PRLR antagonist and oPRL used in these experiments resulted in a functional excess of antagonist. *p*-STAT5 was detected by Western blot in the nuclear fraction of

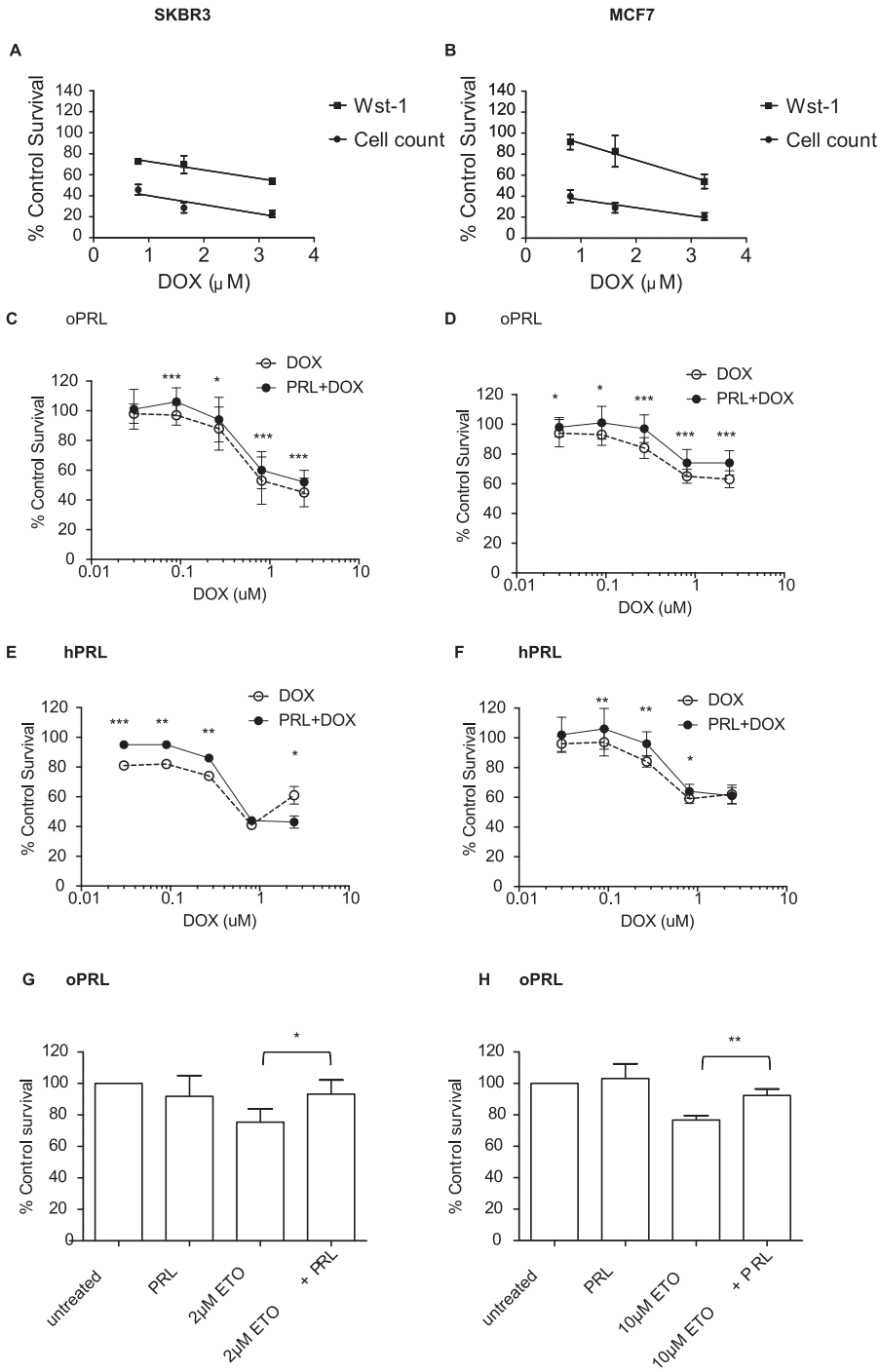

Figure 2. PRL increases cellular viability in the presence of TOPOII poisons. (A) SKBR3 cells or (B) MCF7 cells treated or not with doxorubicin (DOX) were each assessed for viability by either the WST-1 assay or by cell counting. Three independent experiments. (C and E) SKBR3 and (D and F) MCF7 cells were pretreated or not with (C and D) 5 μg/mL oPRL or (E and F) 25 ng/mL hPRL for 24 hours, followed by 2 hours of DOX treatment, with or without PRL, then a 48-hour recovery with or without PRL as indicated in the WST-1 assay. Graphs represent pooled experiments (C) n = 6, SKBR3; (D) n = 5, MCF7; (E) n = 6, SKBR3; (F) n = 12, MCF7. Data were analyzed with a one-way ANOVA followed by Bonferroni posttests. Cell viability (WST-1) assay showing PRL-mediated resistance to etoposide (ETO) treatment in (G) SKBR3 and (H) MCF7 cells. Cells were pretreated or not with 5 μg/mL oPRL for 24 hours followed by 2 hours of ETO treatment at the concentration indicated, then a 48-hour recovery, all in the presence or absence of PRL. Graphs represent six pooled independent experiments. Viability of untreated cell cultures was set to 100%. Student *t* test used in analysis. Error bars represent standard deviations, and they are not visible if smaller than symbol size. Statistically significant analysis: $*P < 0.05$; $**P < 0.01$; $***P < 0.001$.

PRL-treated cells and was barely detected in the nuclear fraction of cells treated with Δ1-9-G129R-hPRL alone or with PRL (Fig. 3B), indicating the PRLR antagonist could compete with oPRL. The results indicate that the PRLR antagonist Δ1-9-G129R-hPRL reduces PRL-JAK2-STAT5 signaling, as a readout of PRLR activation.

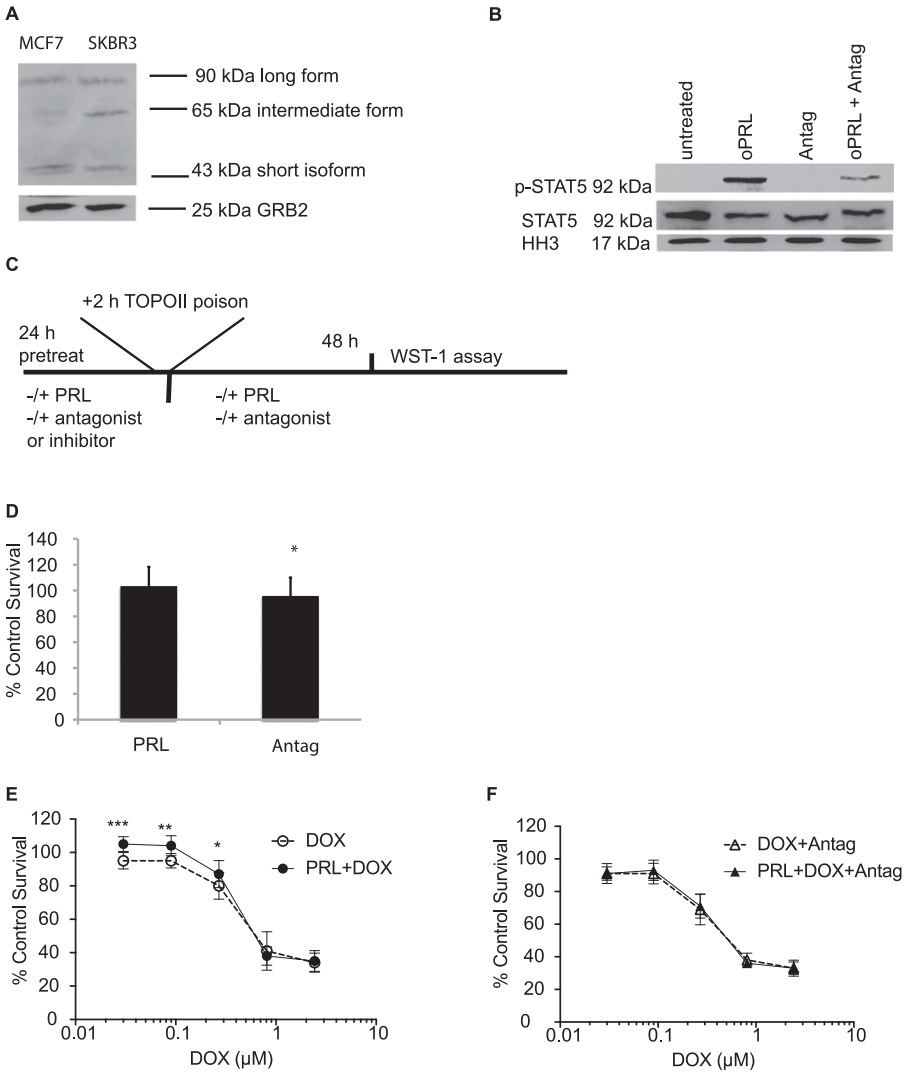

Figure 3. Δ1-9-G129R-hPRL PRLR antagonist abrogates the PRL-mediated increase in SKBR3 cell viability. (A) Western blot of MCF7 and SKBR3 whole cell extracts probed with the anti-PRLR extracellular domain antibody, 1A2B1. (B) Western blot of nuclear extracts (10 μg/well) of SKBR3 cells starved in serum-free media for 16 hours then treated with 5 μg/mL oPRL or 5 μg/mL Δ1-9-G129R-hPRL PRLR antagonist (Antag) for 1 hour or left untreated, probed for *p*-STAT5, STAT5 (rabbit-anti-STAT5), and histone-H3 (HH3) (loading control). (C) A general schematic for treatments used in WST-1 assays including a 24-hour pretreatment, 2 hours of TOPOII poison, followed by a 48-hour recovery period. (D, E, and F) WST-1 assays using SKBR3 cells pretreated or not with 5 μg/mL oPRL ± Δ1-9-G129R-hPRL for 24 hours followed by 2 hours of doxorubicin (DOX) treatment, with or without PRL or Δ1-9-G129R-hPRL, then a 48-hour recovery with or without PRL or Δ1-9-G129R-hPRL as indicated. (D) The effect of oPRL or PRLR antagonist alone. (E) The effect of DOX ± PRL and (F) the effect of DOX + Antag ± PRL. Graphs represents pooled experiments, n = 12. Data were analyzed with a one-way ANOVA followed by Bonferroni posttests. $*P < 0.05$; $**P < 0.01$; $***P < 0.001$.

To test whether the PRLR antagonist Δ1-9-G129R-hPRL prevented the PRL-mediated resistance to doxorubicin, SKBR3 cells were pretreated with oPRL (or vehicle) or Δ1-9-G129R-hPRL (or vehicle) for 24 hours, then 2 hours with increasing concentrations of doxorubicin, with a 48-hour recovery period ± PRL or Δ1-9-G129R-hPRL (Fig. 3C). Viability was assessed by WST-1 assay. The impact of PRL or the PRLR antagonist alone on viability was minimal (Fig. 3D). We observed that PRL increased the viability of cells treated with doxorubicin over the lower concentrations of doxorubicin (Fig. 3E), as expected, but the effect was abrogated in the presence of the PRLR antagonist (Fig. 3F). PRL could not overcome the decrease in cell viability after doxorubicin treatment when in the presence of the PRLR antagonist. Therefore, PRL-mediated resistance to the chemotherapeutic requires activation of the PRLR. We next investigated the downstream molecular mechanism.

HSP90 inhibition abrogates PRL-mediated resistance

Given the roles of HSP90α in cellular survival and as a PRL-STAT5 target gene, its role in PRL-mediated resistance to DNA-damaging agents was investigated. We chose a concentration of 17-AAG that resulted in a ≤20% reduction in viability in both cell lines: 15 nM

in SKBR3 and 100 nM in MCF7. SKBR3 cells were much more sensitive to 17-AAG than MCF7, based on dose-response curves (80). Cells were treated as in Fig. 3C, with 17-AAG added in the pretreatment ± oPRL, followed by 2 hours of doxorubicin treatment, and 48 hours of recovery ± PRL. Individual treatments of PRL and the HSP90 inhibitor 17-AAG, using the WST-1 assay, are shown for SKBR3 (Fig. 4A) and MCF7 (Fig. 4D). PRL

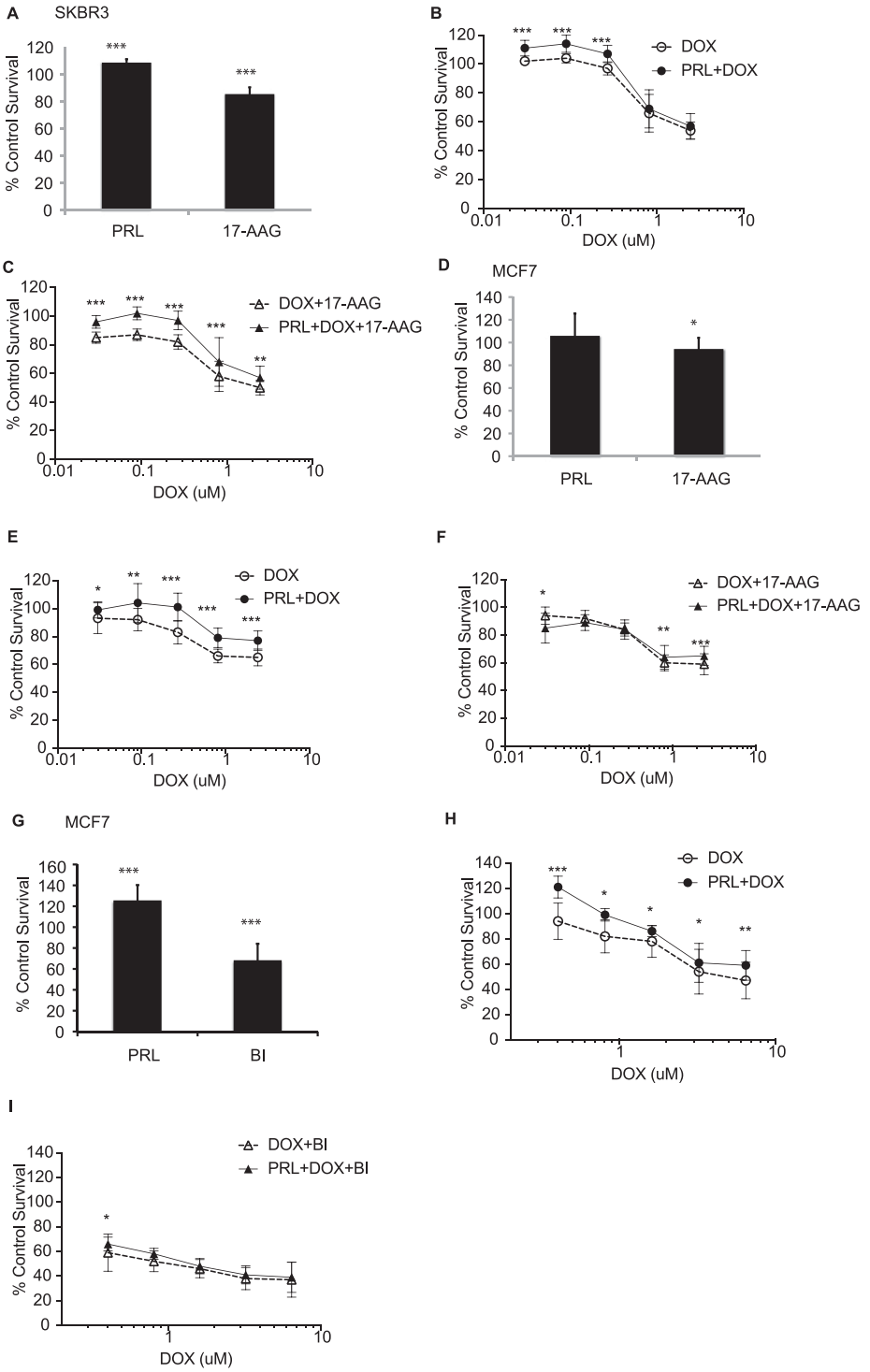

Figure 4. HSP90 inhibition abrogates PRL-mediated resistance. (A, B, and C) SKBR3 or (D, E, and F) MCF7 cells were pretreated or not with 5 μg/mL oPRL, 15 nM (SKBR3) or 100 nM (MCF7) HSP90 inhibitor 17-AAG, or a combination of the two for 24 hours followed by 2 hours of doxorubicin (DOX) treatment, ±PRL or 17-AAG, and a 48-hour recovery ± PRL. (A–C) WST-1 assays of SKBR3 (A) with PRL or 17-AAG alone, (B) with DOX ± PRL, or (C) with DOX + 17-AAG ± PRL. (D–F) WST-1 assays of MCF7 (D) with PRL or 17-AAG alone, (E) with DOX ± PRL, or (F) with DOX + 17-AAG ± PRL. Graphs represent pooled experiments for SKBR3 n = 12, and for MCF7 n = 18. (G–I) WST-1 assays of MCF7 (G) with oPRL or 800 nM BIIB021 alone, (H) with DOX ± PRL, or (I) with DOX + BIIB021 ± PRL. n = 18. Data were analyzed with a one-way ANOVA followed by Bonferroni posttests. $*P < 0.05$; $**P < 0.01$; $***P < 0.001$.

increases cellular viability in the presence of doxorubicin for SKBR3 (Fig. 4B) and MCF7 (Fig. 4E). Although 17-AAG did not interfere with the PRL-mediated increase in survival in SKBR3 cells (Fig. 4C), treatment of MCF7 cells with 17-AAG reduced the PRL-mediated resistance of MCF7 cells to doxorubicin (Fig. 4F). We also tested a second HSP90 inhibitor, BIIB021 (also known as CNF2024), in place of 17-AAG in MCF7 cells. The concentration of 800 nM BIIB021 was chosen (Fig. 4G) based on a dose-response curve (82), and BIIB021 reduced PRL-induced survival. Human PRL increased the viability of doxorubicin-treated cells across all five concentrations (Fig. 4H), but its effect was strongly reduced in the presence of BIIB021 (Fig. 4I). Taken together, these results indicate that HSP90 is involved in the PRL-PRLR–mediated resistance to DNA-damaging chemotherapeutics such as doxorubicin.

JAK2 protein levels decrease with 17-AAG treatment

To test the hypothesis that JAK2 is dependent on HSP90 as a chaperone also in breast cancer cells, MCF7 breast cancer cells were treated or not with the HSP90 inhibitors 17-AAG and BIIB021 in the presence or absence of PRL for 24 hours, followed by 2-hour doxorubicin (0.2 μM) treatment, to replicate the conditions used in our previous experiments (Fig. 3C). Protein levels of JAK2 and the loading control GRB2 were detected by Western blot and quantified. Protein levels of JAK2 decreased with 17-AAG (Fig. 5A and 5B), irrespective of the presence of doxorubicin or PRL, and also decreased

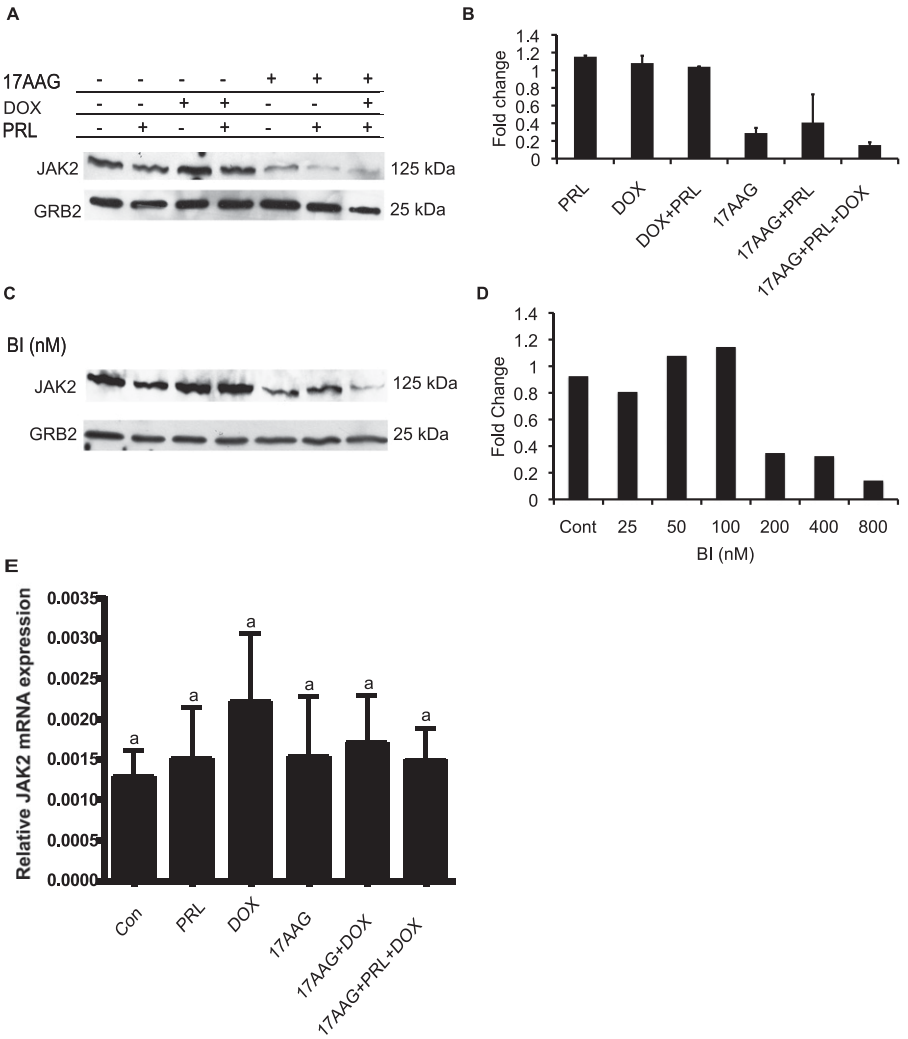

Figure 5. JAK2 protein but not mRNA decreases with HSP90 inhibition. (A) MCF7 cells were pretreated with oPRL (5 μg/mL) and ± 17-AAG (100 nM) for 24 hours followed by doxorubicin (DOX) (0.2 μM) treatment for 2 hours ± PRL. JAK2 and GRB2 levels were detected by Western blot. (B) ImageJ quantification of two pooled experiments. The signal for JAK2 was normalized to that of GRB2, and fold induction was calculated to the untreated control. (C) MCF7 cells were treated or not with BIIB021 (BI). JAK2 and GRB2 levels were detected by Western blot. (D) ImageJ quantification. (E) MCF7 cells were treated as above and RNA extracted. JAK2 expression was compared by qPCR, and the results were normalized to the YWHAZ control [mean ± standard error of the mean (SEM); n = 5]. The $\Delta\Delta$Ct method was used to analyze the relative changes in gene expression. The letter "a" above SEM bars denotes that there were no statistically significant differences (one-way ANOVA followed by Bonferroni posttest, $P < 0.05$).

with BIIB021 treatment (Fig. 5C and 5D). The levels of JAK2 messenger RNA (mRNA) were unaffected by PRL, doxorubicin, 17-AAG, or a combination thereof (Fig. 5E). These data indicate that JAK2 is dependent on HSP90 as a chaperone in breast cancer cells and that JAK2 protein levels are reduced in the presence of HSP90 inhibitors.

JAK2 contributes to PRL-mediated cell viability after DNA damage

To test whether the decrease in JAK2 protein levels and therefore decreased activity affects PRL-mediated cell viability, we used the JAK2 inhibitor G6 (83) in cell viability assays. The inhibition of JAK2 kinase activity was confirmed by Western blot after 12 hours of treatment, with *p*-STAT5 used as a readout. The results showed a decrease in *p*-STAT5 levels starting at 12.5 μM and almost complete inhibition at ≥25 μM (Fig. 6A). Under the conditions established in the Western blot assays, the dose-response of G6 on cell viability was tested with the WST-1 assay. The results showed a significant decrease in cell viability starting at concentrations ≥12.5 μM (Fig. 6B). The concentration (25 μM) of G6 was chosen that inhibited JAK2 activity and resulted in 80% cell viability for the next experiment. To investigate whether JAK2 is involved in the PRL-increased cell viability after DNA-damaging agents, MCF7 and SKBR3 cells were pretreated for 24 hours with 25 ng/mL hPRL and 12 hours with 25 μM G6, followed by 2 hours of doxorubicin treatment, as described in Fig. 3C, but pretreating with G6 for only 12 hours because of the sensitivity of the cells to the inhibitor. Cell viability was determined by a WST-1 assay after 48 hours of recovery time with or without PRL. PRL treatment alone increased the viability and G6 alone reduced viability significantly when compared with the vehicle controls in both MCF7 (Fig. 6C) and SKBR3 cells (Fig. 6F).

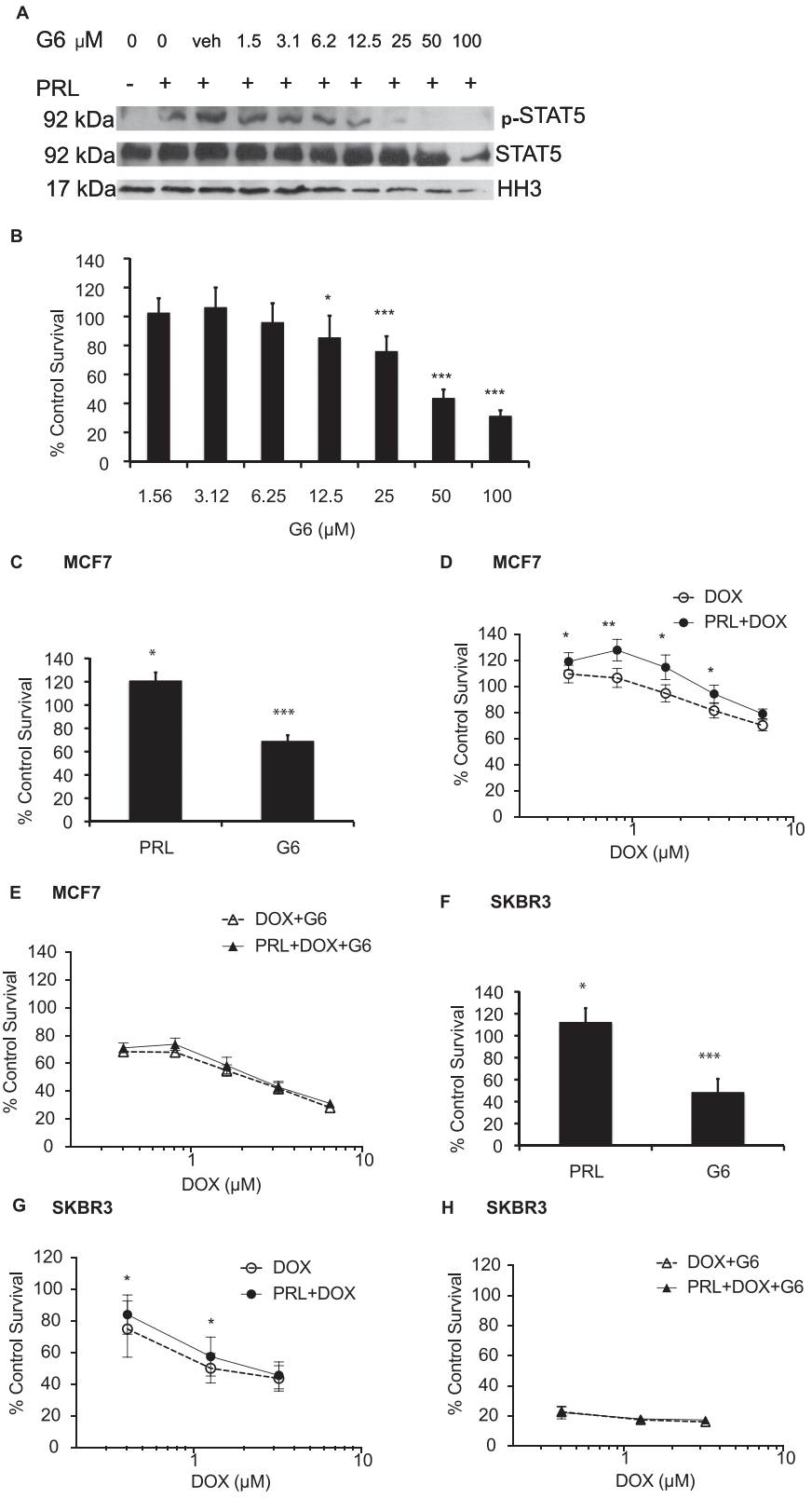

Figure 6. JAK2 inhibition abrogates the PRL increased cell viability. (A) Western blot of JAK2 inhibitor dose response. MCF7 cells were treated with twofold increasing concentrations of G6 for 12 hours. *p*-STAT5 levels were determined (mouse anti-*p*-STAT5) with total STAT5 and histone H3 (HH3) loading controls. Results are representative of two independent experimental replicates. (B) Dose-response curves of JAK2 inhibitor G6. MCF7 cells were treated with G6 at indicated time points and concentrations. The cell viability was determined with WST-1 cell viability assay. WST-1 assays of (C–E) MCF7 or (F–H) SKBR3 cells pretreated with 25 ng/mL hPRL for 24 hours or 25 μM JAK2 inhibitor G6 for 12 hours, followed by

There is a PRL-independent effect of JAK2 on survival. The results showed that PRL increased the cell viability in the presence of doxorubicin in both MCF7 (Fig. 6D) and SKBR3 cells (Fig. 6G), and this increase was completely abolished with JAK2 inhibition in both MCF7 (Fig. 6E) and SKBR3 cells (Fig. 6H). Because PRL cannot overcome JAK2 inhibition, this suggests JAK2 is involved in the PRL-mediated increase in cell viability in doxorubicin-treated breast cancer cells.

p-ATM is dependent on the chaperone HSP90

Given that ATM would probably respond to the double-strand DNA breaks induced by doxorubicin and etoposide, and given the previous reports that ATM was dependent on HSP90 chaperone functions, we tested the stability of *p*-ATM and ATM in the presence of HSP90 inhibitors. MCF7 cells were pretreated or not with 17-AAG at threefold increasing concentrations for 24 hours, followed by 2 hours of 0.2 μM doxorubicin or vehicle, and protein extracts were resolved by sodium dodecyl sulfate polyacrylamide gel electrophoresis (SDS-PAGE) and probed for ATM, *p*-ATM, HSP90α, and GRB2 via Western blotting. There is a small amount of *p*-ATM in MCF7 cells in the absence of exogenously induced DNA damage, perhaps indicative of genomic instability of the cancer cells. The ATM and HSP90α signals were normalized to that of GRB2. Fold change, in the presence of doxorubicin and 17-AAG, was calculated with respect to doxorubicin treatment alone. Total ATM and *p*-ATM levels decreased at 17-AAG concentrations of ≥9 mM (Fig. 7A–7C). Levels of HSP90α were not affected by 17-AAG (Fig. 7A). The levels of ATM mRNA were unchanged by the treatments (Fig. 7D). We also observed a reduction in ATM and *p*-ATM protein levels in DNA-damaged SKBR3 cells upon treatment with the HSP90 inhibitor (Fig. 7E–7G). These results confirm previous reports that ATM and *p*-ATM are dependent on HSP90 in cells that have been exposed to DNA damage.

ATM is involved in PRL-mediated cell viability and clonogenic growth after DNA damage

To investigate whether ATM is involved in PRL-enhanced cell viability, MCF7 and SKBR3 were treated with ATM inhibitor KU55933 at 10 μM, a concentration chosen from the literature where tumor cell lines (e.g., HeLa, PC-3, MDA-MB-463) were tested in conjunction with DNA-damaging chemotherapy agents (e.g., doxorubicin, etoposide) (84). Cells were pretreated with 25 ng/mL hPRL or 10 μM KU55933 for 24 hours followed by 2 hours of doxorubicin treatment. Cells recovered in the absence of doxorubicin and the presence of KU55933 or PRL, consistent with the first treatment conditions for 48 hours (Fig. 3C). PRL alone increased the cell viability and KU55933 alone decreased cell viability significantly when compared with their vehicle controls in both MCF7 (Fig. 8A) and SKBR3 cells (Fig. 8D). PRL increased the viability of doxorubicin-treated MCF7 cells (Fig. 8B) and SKBR3 cells (Fig. 8E), except in the presence of KU55933 in both MCF7 (Fig. 8C) and in SKBR3 cells (Fig. 8F). These data suggest that ATM may be involved in the mechanism of PRL-mediated increase in cell viability.

To confirm our findings, we used siATM in assays that test clonogenic growth. To optimize conditions and determine knockdown efficiency, MCF7 and SKBR3 cells were transfected with siATM or with siNT. According to relative gene expression quantification, ATM gene expression was knocked down >90% by 72 hours in MCF7 (Fig. 9A) and by 48 hours in SKBR3 cells (Fig. 9C). At the protein level, ATM was greatly reduced by 48 hours after transfection and remained low at 96 hours after transfection in both cell lines (Fig. 9B and 9D).

Based on the ATM gene knockdown results, a clonogenic assay was designed as follows: MCF7 and SKBR3 cells were transfected with siNT or siATM. At 48 hours after transfection, cells were treated or not with 25 ng/mL hPRL, and 24 hours later cells were treated with doxorubicin for 2 hours. Cells were then counted and transferred to six-well plates with fresh media, with or without PRL, and allowed to form colonies over 10 to 15 days. In the presence of siNT, PRL increased the survival of doxorubicin-treated cells significantly in both MCF7 (Fig. 9E) and SKBR3 (Fig. 9G) cells. However, in cells transfected with siATM, PRL was unable to increase the clonogenic survival of MCF7 (Fig. 9F) or SKBR3 (Fig. 9H) cells, with a greater effect in the SKBR3 cells. The results overall indicate that ATM is needed for the PRL-mediated increase in clonogenic cell survival, as well as cell viability, in breast cancer cells after DNA damage.

Doxorubicin synergizes with the HSP90 inhibitor BIIB021 and also with KU55933

Given our observations that the combination of BIIB021 and doxorubicin (Fig. 4H and 4I) or KU55933 and doxorubicin (Fig. 8B, 8C, 8E, and 8F) strongly reduced cell viability compared with the drugs alone, we investigated the nature of the interaction between drugs by using CompuSyn to calculate the median effect and CI. We first evaluated the nature of the interaction between doxorubicin and KU55933 in the concentration range

Figure 6. (Continued). 2 hours doxorubicin (DOX) treatment with or without PRL or G6 and 48-hour recovery period in the presence or absence of PRL. (C–E) MCF7 cells treated with (C) PRL or G6 alone, (D) DOX ± PRL, or (E) DOX + PRL ± G6. (F–H) SKBR3 cells treated with (F) PRL or G6 alone, (G) DOX ± PRL, or (H) DOX + PRL ± G6. Results represent 18 pooled experiments (n = 18). One-way ANOVA followed by Bonferroni test. $*P < 0.05$; $**P < 0.01$; $***P < 0.001$.

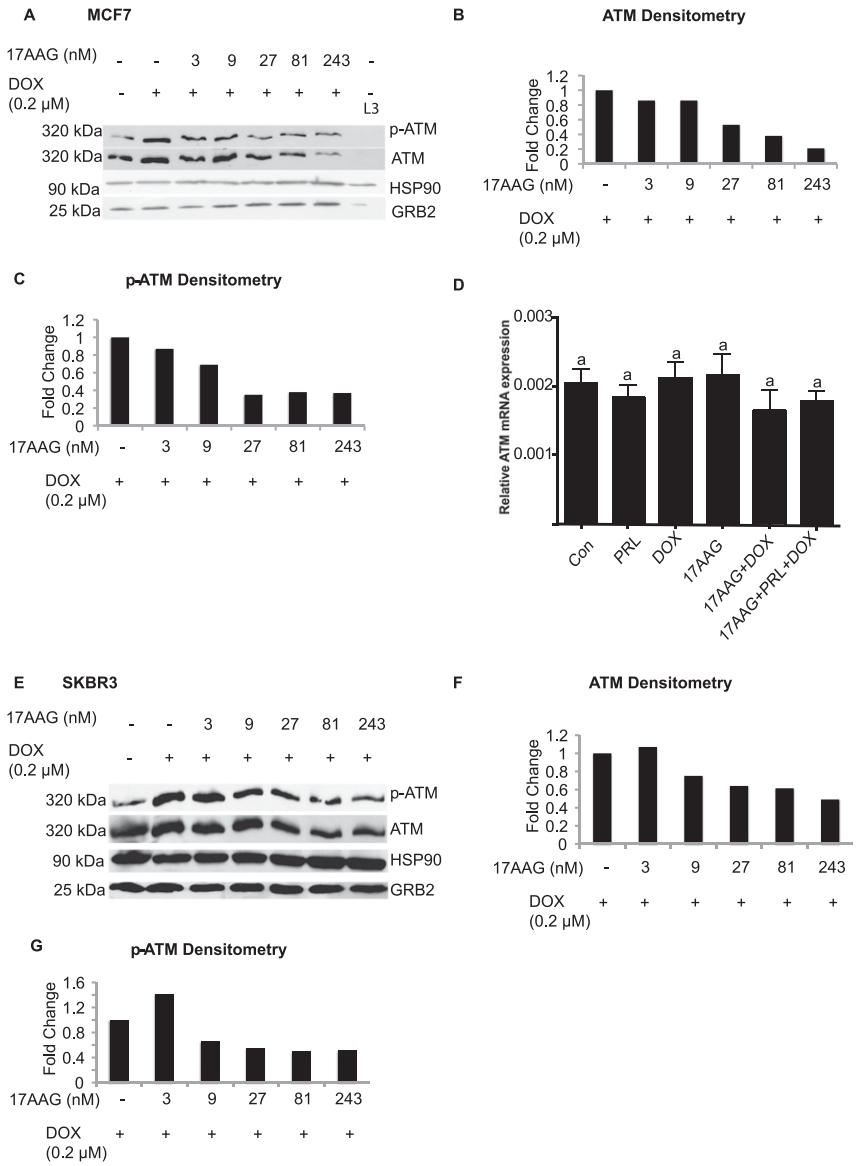

Figure 7. HSP90 inhibition decreases ATM and *p*-ATM protein but not its mRNA. (A) MCF7 cells were treated or not with threefold increasing concentrations of 17-AAG for 24 hours followed by 2 hours of doxorubicin (DOX) treatment and recovery. Proteins (30 μg per well) were resolved on SDS-PAGE gel, and blot was probed for *p*-ATM, ATM, HSP90α, and GRB2. Gel is representative of two experiments. Fold difference of *p*-ATM with DOX treatment was calculated, in ImageJ, compared with untreated cells (set to 1). Fold difference of (B) total ATM and (C) *p*-ATM levels with 17-AAG and DOX treatment were calculated compared with DOX alone (set to 1). Representative blot of two experiments. (D) MCF7 cells were pretreated with oPRL (5 μg/mL) or 17-AAG for 24 hours, followed by 2 hours DOX treatment (0.2 μM). ATM expression was detected by qPCR, and the results were normalized to YWHAZ control [mean ± standard error of the mean (SEM); n = 5]. The $\Delta\Delta$Ct method was used to analyze the relative changes in gene. The letter "a" above SEM bars denotes that there were no statistically significant differences (one-way ANOVA followed by Bonferroni test, $P < 0.05$). (E) SKBR3 cells as above, with (F) ATM and (G) *p*-ATM band intensities quantified by ImageJ. Representative blot of two experiments.

used in the experiments, using CompuSyn. The cytotoxicity of doxorubicin and KU55933 was tested on MCF7 breast cancer cells with a WST-1 cell viability assay, and the half minimal (50%) inhibitory concentration values were calculated as 5 μM for doxorubicin and 30 μM for KU55933 (Fig. 10A). Based on this dose response, two concentrations of KU55933 (10 and 20 μM) that reduced cell viability ~20% to 25% were chosen to use as fixed concentration in calculations where doxorubicin was used in threefold increasing concentrations (Fig. 10B). The results show that there is moderate to full synergism between doxorubicin and KU55933 in the low range of drug doses and slight to moderate synergism at the highest dose of doxorubicin used in our experiments (Fig. 10C and Table 1).

Inhibition of HSP90 has been shown to sensitize cells to radiation (56, 85, 86) and doxorubicin-induced DNA damage (87). Based on our observations that BIIB021 and doxorubicin together strongly reduced cell viability compared with the drugs alone, we investigated this

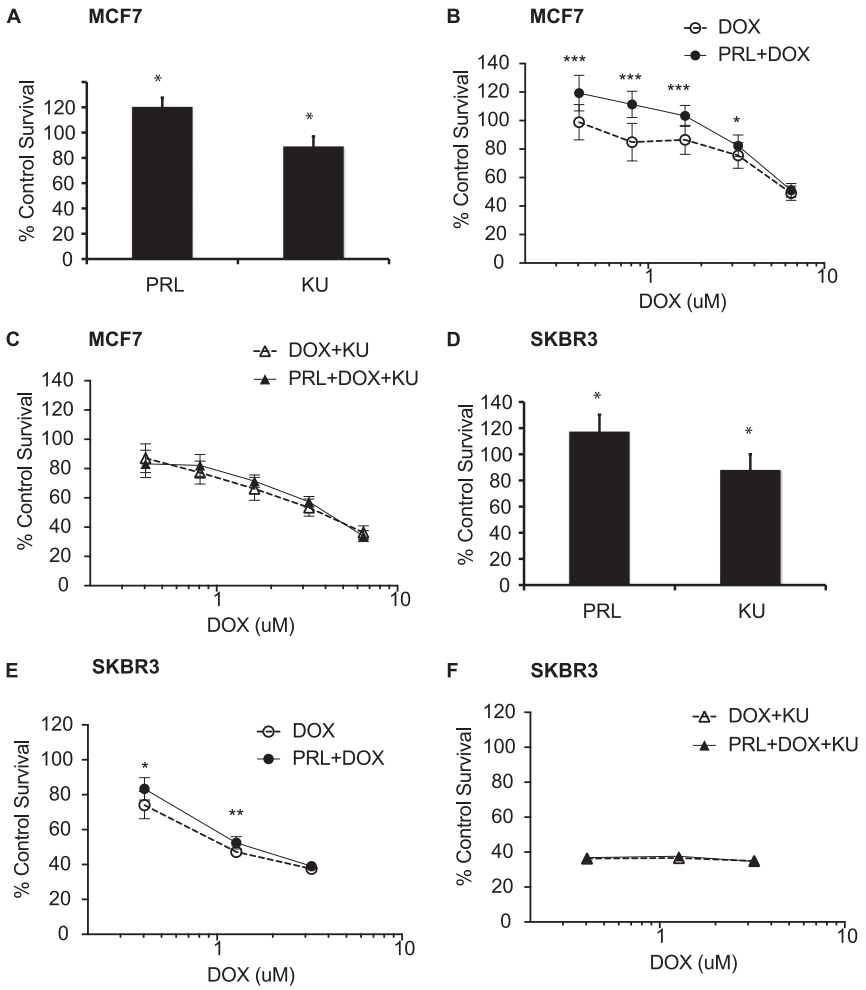

Figure 8. ATM inhibition abrogated the PRL-increased cell viability. MCF7 or SKBR3 cells were pretreated with 25 ng/mL hPRL, 10 μM ATM inhibitor KU55933 (KU), or a combination of the two for 24 hours. This was followed by 2 hours of doxorubicin (DOX) treatment with or without PRL or KU and a 48-hour recovery period with or without KU or PRL. Cell viability was determined with a WST-1 assay, and all treatments were normalized to vehicle controls. (A) Single hPRL and KU treatments in MCF7 cells. Combination treatments with (B) DOX ± hPRL or (C) DOX + KU ± PRL in MCF7 cells. (D) Single hPRL and KU treatments in SKBR3 cells, (E) DOX ± hPRL, or (F) DOX + KU ± PRL in SKBR3 cells. All results represent pooled experiments (n = 18). Data were analyzed with a one-way ANOVA followed by Bonferroni posttests. $*P < 0.05$; $**P < 0.01$; $***P < 0.001$.

further by using the same viability assays testing the HSP90 inhibitor BIIB021 and doxorubicin in MCF7 cells. Based on dose response curves (Fig. 10D), the concentrations of BIIB021 (400 nM and 800 nM) that reduced cell viability ~20% to 25% were chosen as fixed concentrations in calculations, where doxorubicin was used in threefold increasing concentrations (Fig. 10E). CI results show that there is full to strong synergism between doxorubicin and BIIB021 at the lower concentrations and slight to full synergism at the highest concentration of doxorubicin (Table 2 and Fig. 10F).

PRL requires ATM for promoting cell survival after DNA damage in 3D culture

To determine whether our observations extended into 3D cell culture as a more relevant model, we assessed the cellular responses in 3D collagen type I gel culture. To limit exposure to doxorubicin consistent with our previous assays, we plated and treated SKBR3 and MCF7 cells in two-dimensional (2D) cultures with PRL or vehicle for 24 hours, followed by 2 hours of doxorubicin or vehicle treatment before trypsinizing and replating the cells into 3D collagen gels and allowing cells to recover in the presence of hPRL or vehicle. We also observed that PRL was still able to induce cell viability in doxorubicin-treated cells (Fig. 11A and 11B), consistent with the results in 2D.

Using siATM, we observed that PRL lost its ability to increase cell viability of doxorubicin-treated SKBR3 (Fig. 11C and 11E) or MCF7 cells (Fig. 11D and 11F), compared with cells transfected with siNT. This is consistent with our observations in 2D cultures and indicates that ATM is needed for the PRL-mediated increase in cell viability after DNA damage.

Discussion

We have demonstrated that the PRL–PRLR–JAK2–STAT5–HSP90 pathway increases the viability of cells treated with DNA-damaging agents, such as doxorubicin, in both 2D and 3D culture, and that this effect is dependent on functional ATM. ATM was also needed for the ability of PRL to promote clonogenic survival after DNA damage. This effect is specific to the PRLR, as assessed by using the PRLR antagonist Δ1-9-G129R-hPRL. We also showed that HSP90 helps mediate this effect, because ATM is dependent on HSP90 for maturation and JAK2 for maturation or stability, and thus HSP90 links the two pathways of PRL signaling and the DNA damage response (Fig. 12).

We observed differences between the cell lines, in that MCF7 cells were dependent on HSP90 for PRL-mediated increase in viability, whereas SKBR3 cells were not. This finding could indicate that there is a necessary but unidentified HSP90 client in MCF7 cells that depends on HSP90 for stability rather than maturation. Certain HSP90 client proteins are more sensitive to HSP90 inhibitors than other client proteins, and this sensitivity may depend on whether the client protein relies on

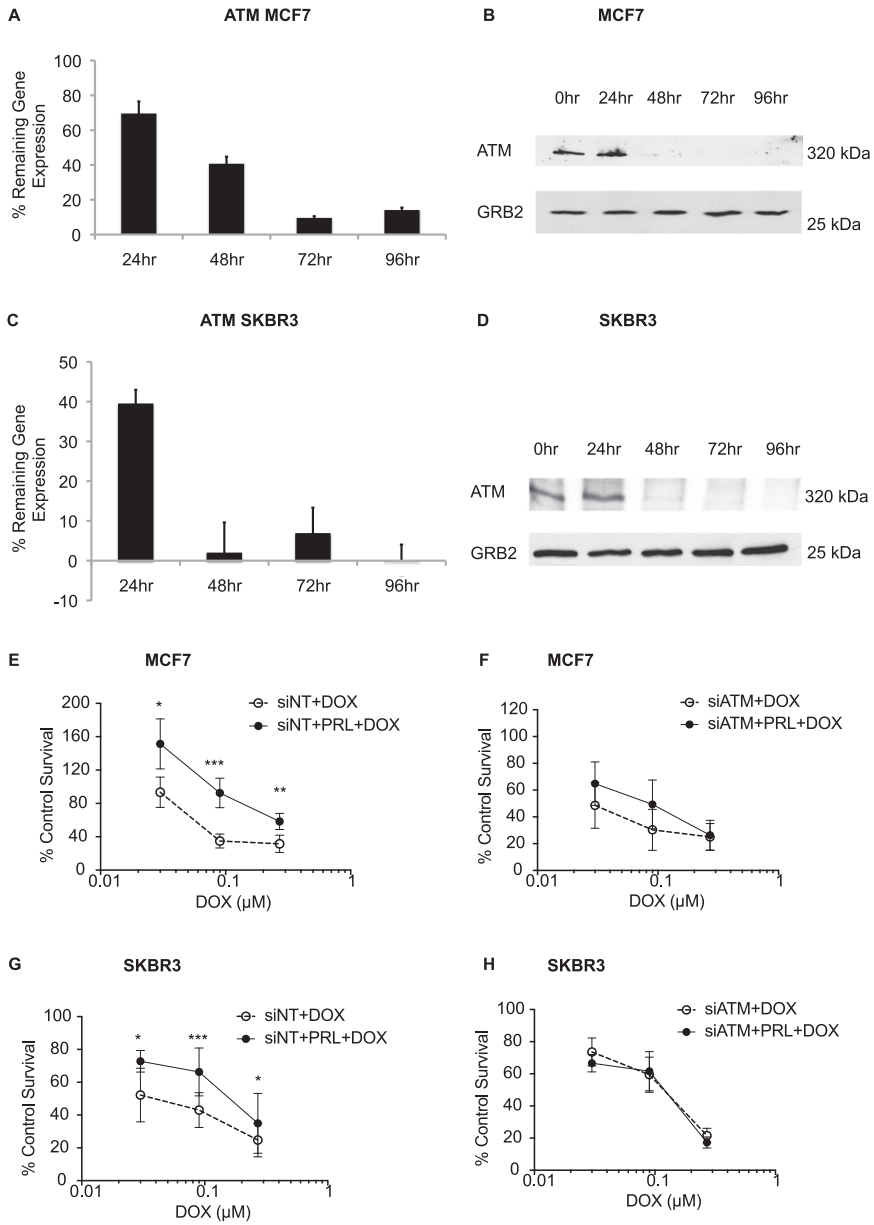

Figure 9. siRNA-mediated silencing of ATM prevents PRL-mediated clonogenic survival after doxorubicin (DOX) treatment. MCF7 and SKBR3 cells were transfected with siATM or with siNT. Relative gene expression was determined with $\Delta\Delta$Cq from qPCR data, with YWHAZ as reference gene. Percentage gene expression was calculated by normalizing data to the reference gene, followed by calculating the percentage of gene expression compared with the nontargeting control. (A) Knockdown of ATM gene over 96 hours in MCF7 cells. (B) Western blot showing loss of ATM protein over 96 hours in MCF7 cells. (C) Knockdown of ATM gene over 96 hours in SKBR3 cells. (D) Western blot showing loss of ATM protein over 96 hours in SKBR3 cells. MCF7 and SKBR3 cells were transfected with siATM or siNT followed by 24 hours of 25 ng/mL PRL treatment and 2 hours DOX treatment. Cells were transferred to six-well plates to allow colony formation. All treatments were normalized to vehicle or siNT controls. (E and F) Clonogenic cell survival in (E) siNT-transfected or (F) siATM-transfected MCF7 cells. (G and H) Clonogenic cell survival in (G) siNT-transfected or (H) siATM-transfected SKBR3 cells. Results represent six pooled experiments (n = 6). Data were analyzed with a one-way ANOVA followed by Bonferroni posttests. $*P < 0.05$; $**P < 0.01$; $***P < 0.001$.

HSP90 for synthesis (maturation) or for continued stability. When a client protein relies on HSP90 for continued stability, the inhibition of HSP90 would be similar to inhibition of their synthesis, and their degradation would relate to their half-life. In this case, as with ATM and possibly JAK2, there is enough protein remaining to carry out their function under the conditions we have used. Another caveat is the occupation of HSP90 by the inhibitor, and given the concentrations and treatment times used in this study, we may have <100% occupancy in both cell lines and less occupancy in the SKBR3 cells compared with the MCF7 cells (88).

The difference in sensitivity of SKBR3 and MCF7 to 17-AAG may occur for two reasons. One reason lies in their differing abilities to undergo apoptotic death, because 17-AAG induces a caspase-3–mediated cell death via BAX (89), whereas MCF7 cells do not produce caspase-3 and do not undergo BAX-mediated nuclear fragmentation, although they still undergo BAX-induced cell death (90). A second reason may be the difference in BRCA1 status; SKBR3 has lower BRCA1 expression than MCF7 cells (91). Cells with low or no BRCA1 are hypersensitive to HSP90 inhibitors such as 17-AAG and undergo mitotic catastrophe (53). These differences in cellular response are possible reasons for the differences in the role of HSP90 in the PRL-mediated viability after DNA damage, in that MCF7 may also rely on a different HSP90 client in the PRL response to overcome DNA damage. Despite these differences, both cell lines relied on PRL-PRLR-JAK2 and the ATM response pathways for cell viability and their clonogenic survival after DNA damage.

The PRLR activates a number of different downstream signaling pathways (92), which may contribute to cell survival. The PRL-PRLR-JAK2 pathway is implicated in the PRL-mediated increase in viability in response to DNA-damaging agents, because we demonstrated that HSP90 inhibition resulted in markedly decreased JAK2 levels, and JAK2 inhibition also abrogated the PRL-mediated resistance to DNA-damaging agents. Although we observed an intrinsic effect of JAK2 inhibition on cell survival, we also observed that PRL depends on JAK2 to increase cell survival after

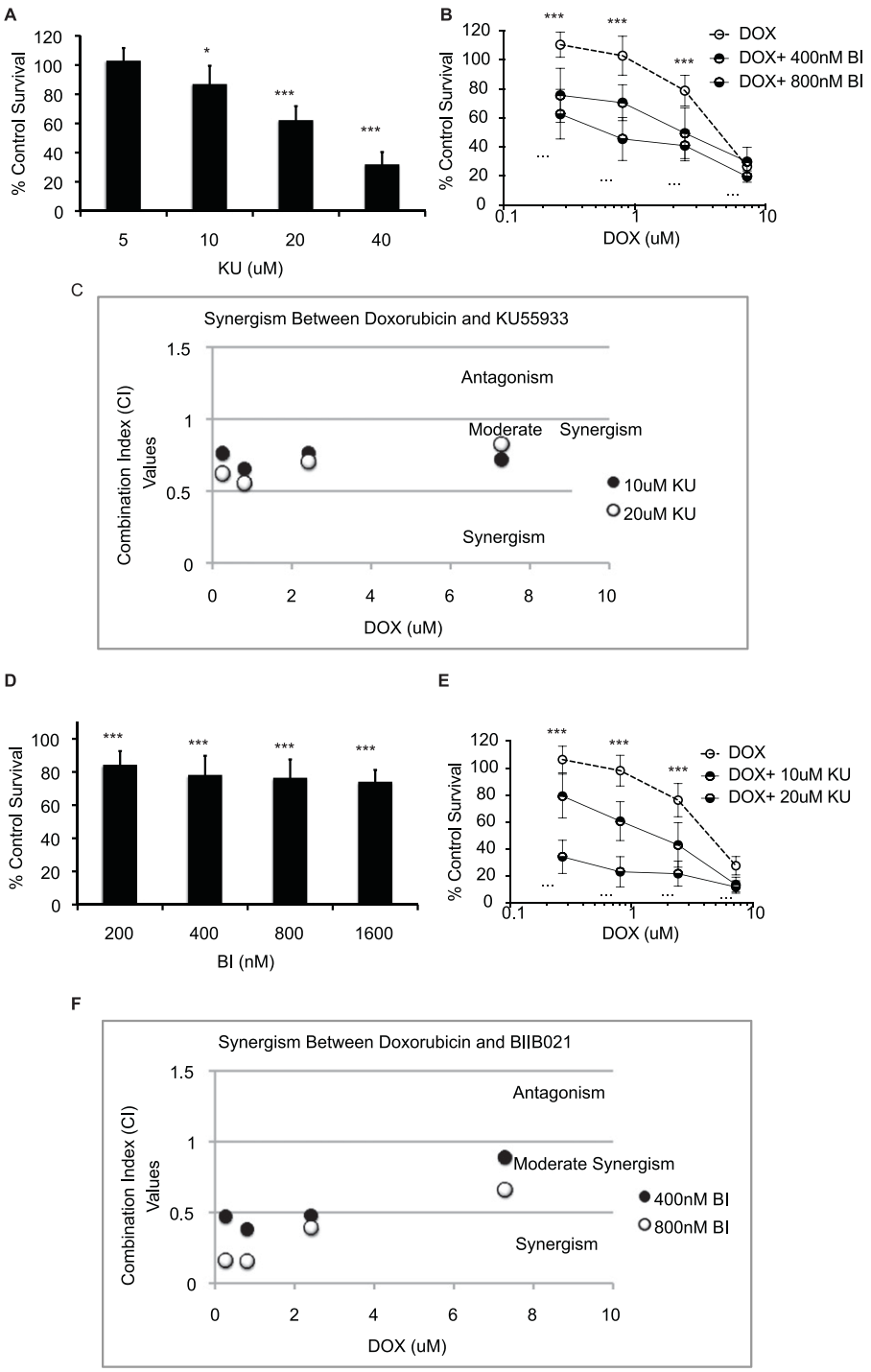

Figure 10. HSP90 inhibitor BIIB021 (BI) and ATM inhibitor KU55933 (KU) synergize with doxorubicin (DOX). Cell viability was determined with WST-1 cell viability assays. (A) KU dose response at 24 hours in MCF7 cells. (B) MCF7 cells were pretreated with KU (10 μM or 20 μM) for 24 hours followed by 2 hours of DOX treatment and 48 hours of recovery, and the treatments were normalized to vehicle control. (C) CI values for DOX and KU. CI < 1, synergism; CI = 1, additive effect; CI > 1, antagonism. Error bars are smaller than symbol size and hence are not visible. (D) BI dose response at 24 hours in MCF7 cells. (E) MCF7 cells were pretreated with BI (400 nM or 800 nM) for 24 hours followed by 2 hours of doxorubicin treatment and 48 hours of recovery, and the treatments were normalized to vehicle control. (F) CI values for DOX and BI. Error bars are smaller than symbol size and hence are not visible. Error bars represent standard deviation from the mean. Results represent nine pooled experiments (n = 9). Statistically significant difference between DOX and DOX + 10 μM KU, or with DOX + 400 nM BI, is marked above each point with an asterisk. Statistically significant difference (in B and E) between DOX and DOX + 20 μM KU or DOX + 800 nM BI is marked below each point with a filled square. *$P < 0.05$; **$P < 0.01$; ***$P < 0.001$. Data were analyzed with a one-way ANOVA followed by Bonferroni posttests.

doxorubicin treatment. JAK2 is shared by many cytokine receptors (93), and JAK2-STAT signaling is known to contribute to cell survival (94, 95).

The fact that HSP90 inhibition leads to JAK2 loss in breast cancer cells is also interesting, given its potential role in PRL-induced mammary cancer initiation but not

Table 1. CI Values From Drug Combination Studies of Doxorubicin With KU55933

Fixed Inhibitor Concentrations	Doxorubicin Concentration (μM)	CI Values	Type of Synergism
KU55933 (10 μM)	0.27	0.75952 ± 0.1629	Moderate synergism
	0.81	0.65443 ± 0.1445	Synergism
	2.43	0.7633 ± 0.1650	Moderate synergism
	7.29	0.71625 ± 0.0551	Moderate synergism
KU55933 (20 μM)	0.27	0.61971 ± 0.1229	Synergism
	0.81	0.55185 ± 0.1125	Synergism
	2.43	0.70035 ± 0.093	Moderate synergism
	7.29	0.82405 ± 0.0459	Slight synergism

Values are mean ± standard deviation of nine experiments.

maintenance (96, 97). However, JAK2 mediates signals not only from the PRLR but also from the growth hormone receptor, which is also associated with lymph node metastasis in breast cancer (26). JAK2 also activates STAT3 (98–100), which is increasingly being recognized for its contributions to breast cancer (101). STAT3 is constitutively activated in ≤60% of breast cancers (102, 103), and it increases tumor growth and increases the metastatic potential of ERBB2 expressing cells (104). JAK2/STAT3 signaling is also necessary for the growth of stem cell–like $CD44^+/CD24^-$ breast cancer cells (105). Therefore, the targeting of JAK2 by HSP90 inhibitors in patients with breast cancer is important on many fronts.

The results also point to the potential involvement of the JAK2-STAT5 pathway in mediating the PRL response in breast cancer cells treated with DNA-damaging agents and further supports the identification of HSP90 as part of this signal pathway and function. The promoter of the HSP90α gene contains at least two potential STAT binding elements, which can bind STAT-1, STAT-3, or STAT5, and reporter assays with the promoter indicated that it preferentially was activated by STAT5B (30). This finding is consistent with the involvement of the JAK2-STAT5B-HSP90α pathway in mediating PRL-induced viability.

Our observation is that PRL-activated JAK2 activation is involved in cellular viability after chemotherapeutic agents, which implicates a role in the cellular resistance to cancer treatment. JAK2 activation of STAT5A downstream of the PRLR has been otherwise associated with differentiation and reduced cellular invasion in breast cancer cells [for discussion and references therein, see (106)], which supports a protective role for the pathway. It may be that in the context of DNA damage, as induced here by chemotherapeutic drugs, the role of JAK2 favors cellular survival.

STAT5B activation, on the other hand, has been demonstrated to be key to the activation of ATM-dependent DNA damage signaling in human papilloma virus–infected cells (107). The human papilloma virus protein E7 activated STAT5B to promote viral replication. The mechanism by which STAT5B activated ATM was indirect, and the authors demonstrated the importance of the STAT5-mediated transcriptional induction of the peroxisome proliferator–activated receptor γ (PPARγ). PPARγ was key in the activation of ATM and the ATM DNA damage response after infection. Although we did not observe a PRL-induced phosphorylation of ATM in the absence DNA damage (82), it would be interesting to test the involvement of PRL-STAT5B-PPARγ as part of this mechanism.

PRL has been recently implicated in breast cancer cell resistance to cisplatin, vinblastine, taxol (32, 33), and ceramide (25), but only a mechanism for cisplatin

Table 2. CI Values From Drug Combination Studies of Doxorubicin With BIIB021

Fixed Inhibitor Concentrations	Doxorubicin Concentration (μM)	CI Values	Type of Synergism
BIIB021 (400 nM)	0.27	0.4685 ± 0.1864	Synergism
	0.81	0.37933 ± 0.1237	Synergism
	2.43	0.47691 ± 0.1750	Synergism
	7.29	0.88603 ± 0.0990	Slight synergism
BIIB021 (800 nM)	0.27	0.1584 ± 0.171	Strong synergism
	0.81	0.15167 ± 0.1488	Strong synergism
	2.43	0.3889 ± 0. 104	Synergism
	7.29	0.65919 ± 0.039	Synergism

Values are mean ± standard deviation of nine experiments.

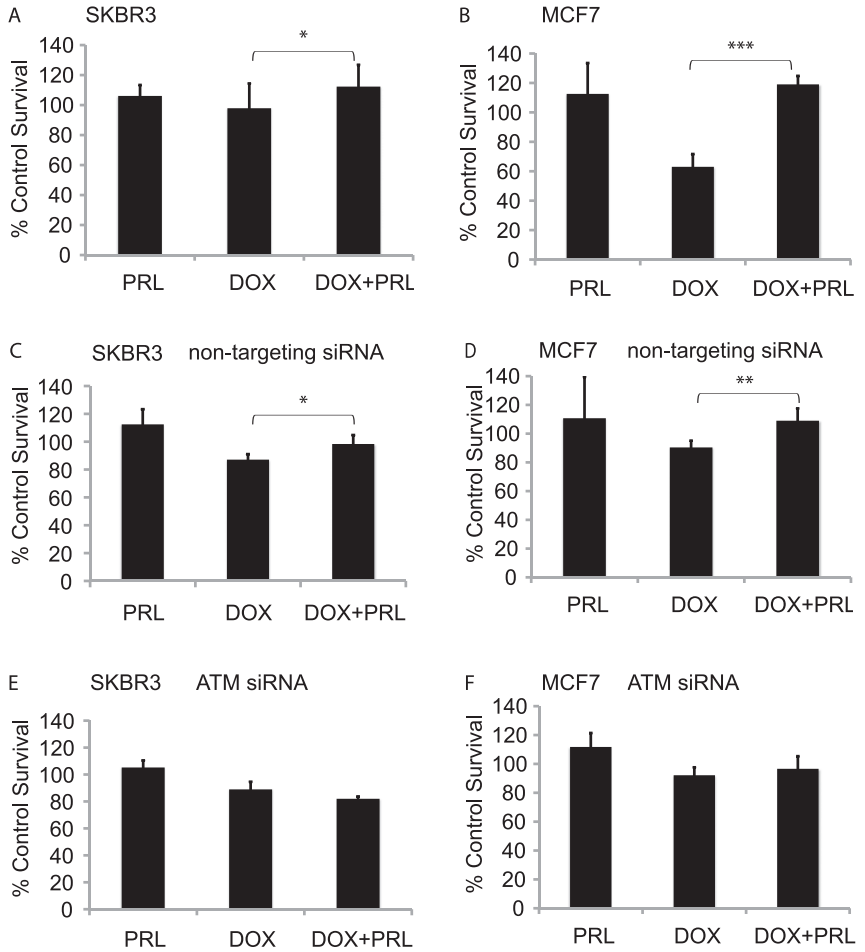

Figure 11. ATM is needed for PRL-induced increase in cell viability after DNA damage in 3D culture. Cells were pretreated with 25 ng/mL hPRL or vehicle for 24 hours followed by 2 hours of 1 μM doxorubicin (DOX) treatment (or vehicle) with or without PRL. Cells were transferred to collagen 3D culture and allowed to recover for 48 hours. Cell viability was determined with WST-1 assay, and the treatments were normalized to vehicle controls: (A) SKBR3 or (B) MCF7. For ATM knockdown experiments, (C and E) SKBR3 and (D and F) MCF7 cells were transfected with (C and D) siNT or (E and F) siATM, followed by 24 hours of 25 ng/mL hPRL and 2 hours of DOX treatment (3 μM for SKBR3, 2 μM for MCF7 cells). Cells were transferred to collagen gels to allow recovery for 96 hours (SKBR3) or 48 hours (MCF7). Bars in the graphs represent six independent experiments. Statistically significant analysis by ANOVA: $*P < 0.05$; $**P < 0.01$; $***P < 0.001$.

resistance has been reported and involves a different PRL target gene, glutathione-*S*-transferase mu1 (32). HSP90β was shown to chaperone the protein product of the rat GSTmu1 gene (108), and the gene encoding HSP90β has also been identified as PRL regulated in the mouse mammary gland (109). It may indicate that the PRL-mediated mechanism for cisplatin resistance also involves HSP90. Global transcriptomic studies have highlighted that PRLR overexpression at the mRNA level is associated with the worst prognosis after treatment with anthracyclines (*e.g.*, doxorubicin) (110), strongly supporting our observations and general hypothesis that PRL is an important factor in the etiology of breast cancer and in its resistance to anticancer therapies.

HSP90 is known to have a number of different client proteins involved in survival and DNA repair, such as the oncogene AKT (111) and other clients involved in cell cycle control [Wee1 (112)], double-strand DNA break repair [MRN complex (56), RAD51 (113)], and single-strand DNA break repair [CHK1 (54)]. We did observe synergism of BIIB021 treatment with doxorubicin, consistent with what was reported for etoposide and 17-AAG in colon cancer cells (114). HSP90 inhibitors such as 17-AAG and BIIB120 have also been demonstrated to sensitize cells to the double-strand breaks of irradiation (115, 116). Inhibition of HSP90 is associated with reduction in homologous repair (53, 117).

Although we cannot rule out that the PRL response may simply not have been able to overcome the toxicity induced by the combination of the JAK2 inhibitor or the ATM inhibitor and doxorubicin, we also observed synergism that would indicate that these pathways are in parallel. We observed synergism between doxorubicin with the HSP90 inhibitor BIIB021 and also doxorubicin with the ATM inhibitor KU55933. The combinatorial drug function highlights the interaction of these molecular pathways, with HSP90 and ATM in parallel pathways (Fig. 12). This interaction defines a crosstalk of the PRL-PRLR pathway with the DNA damage response that increases cell viability and clonogenic survival despite DNA damage.

A possible role for the phosphorylated form of HSP90α in maintaining DNA repair foci, after double-strand DNA damage, was recently identified (118). HSP90α was phosphorylated in response to DNA damage induced by irradiation and recruited to DNA repair foci. This study demonstrated that HSP90α was important for efficient DNA repair, in particular of more persistent lesions. The reduction of HSP90α by RNA silencing or chemical inhibition also resulted in a decrease in cell survival. Therefore, HSP90 is potentially involved in the double-strand DNA damage response and repair, probably via its chaperoning ability. HSP90 is intricately involved in different DNA damage

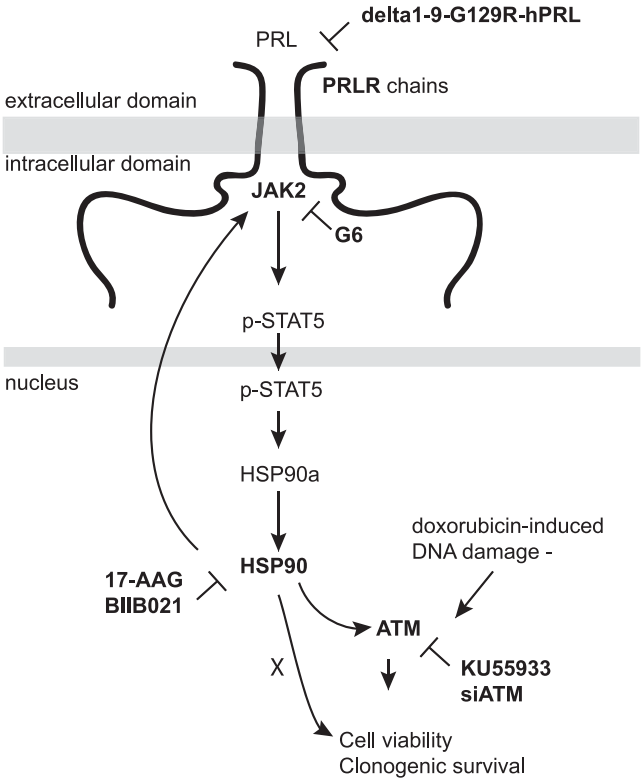

Figure 12. PRL-JAK2-STAT5-HSP90 contributes to resistance to DNA-damaging agents in breast cancer cells. PRL increases breast cancer cell viability and clonogenic survival in cells treated with the DNA-damaging agent doxorubicin, in a mechanism that involves HSP90 and its potential client proteins JAK2 and ATM. PRL binds to its receptor, activating JAK2 kinase, and JAK2 phosphorylates receptor tyrosines that subsequently become docking sites for STAT5 proteins. Activated *p*-STAT5 translocates to the nucleus and activates HSP90A gene transcription. HSP90A protein, in a HSP90 complex, stabilizes JAK2 and ATM. An unknown HSP90 client that may contribute is indicated by an *X*. Shown are the PRLR antagonist, the inhibitors, and siRNA used to interrogate the mechanism.

response pathways, by chaperoning XRCC1 (52), DNA-dependent protein kinase catalytic subunit (57), BRCA1 (53), CHK1 (54), ATR (55), MRN complex (56), and ATM (57). ATM has been shown to be responsible for phosphorylating HSP90α after DNA damage (119). ATM may contribute in a number of ways to cell survival after double-strand DNA damage, such as homologous DNA repair (120).

We observed that ATM was phosphorylated at serine-1981 at all concentrations of doxorubicin or etoposide treatment in SKBR3 cells, and cytotoxicity was evident at each of those doses. It is known that doxorubicin induces double-strand (predominantly) and single-strand DNA breaks at the low concentrations used in this study (121). It is also known that doxorubicin induces breaks linearly over the 2-hour time period and also continues to induce DNA damage after its removal (121). There is not a simple correlation between DNA damage and doxorubicin cytotoxicity. Cytotoxicity for etoposide is related to the double-strand breaks that it induces, which are in the minority compared with its induction of single-strand DNA breaks. KU55933 has been shown to sensitize cells to the topoisomerase II inhibitors etoposide, doxorubicin, and amsacrine in HeLa cells, which supports our finding (122).

Conclusions

We have demonstrated that PRL-induced activation of PRLR signaling mediates cellular resistance to the DNA-damaging agents doxorubicin and etoposide, drugs critical for the treatment of breast cancer. We observed pathway interactions based on the drug synergy between doxorubicin and the ATM inhibitor KU55933, and doxorubicin with the HSP90 inhibitor BIIB021. We also observed that ATM was necessary for the PRL-induced clonogenic survival after DNA damage. We have identified a molecular mechanism that involves the PRL-PRLR-JAK2-STAT5-HSP90 pathway and the ATM-based DNA damage response pathway.

Acknowledgments

We thank Dr. Antoine Angelergues for critical reading of the manuscript and Sara Mirzaei for technical assistance with the gene expression data.

Financial Support: C.S.S.: Natural Sciences and Engineering Research Council of Canada Grant 250185-2010; Ö.K.A.: Natural Sciences and Engineering Research Council of Canada graduate student award; C.S.S., A.U., Ö.K.A.: Alberta Cancer Foundation Grants 22435 and 23135; C.S.S., S.G.G.: The Canadian Breast Cancer Foundation [Canadian Cancer Society Grant 300072]; V.G., F.B.: La Ligue Contre le Cancer, Comité de Paris Grant RS09/75-72. The funders had no role in study design, data collection and interpretation, or the decision to submit the work for publication.

Author Contributions: Ö.K.A., A.U., and S.G. contributed to the experimental data and wrote part of the manuscript. F.B. prepared the recombinant prolactin receptor antagonist and human prolactin. V.G. developed the prolactin receptor antagonist, contributed to the design of experiments involving the latter, and contributed to the manuscript. C.S.S. conceived and designed the experiments, secured funding, and wrote the manuscript.

Correspondence: Carrie S. Shemanko, PhD, Department of Biological Sciences and the Arnie Charbonneau Cancer Institute, 2500 University Drive NW, University of Calgary, Calgary, Alberta T2N 1N4, Canada. E-mail: shemanko@ucalgary.ca.

Disclosure Summary: The authors have nothing to disclose.

Appendix. Antibody Table

Peptide/Protein Target	Antigen Sequence (if Known)	Name of Antibody	Manufacturer, Catalog No.	Species Raised in; Monoclonal or Polyclonal	Dilution Used	RRID
Prolactin receptor ECD	ECD	Prolactin receptor monoclonal antibody (1A2B1)	ThermoFisher Scientific, 35-9200	Mouse; monoclonal	1:1000	AB_2533231
GRB2		Mouse anti-GRB2 monoclonal antibody, unconjugated, clone 81	BD Biosciences, 610111	Mouse; monoclonal	1:5000	AB_397517
Phospho-STAT5		Rabbit anti-STAT5, phospho (Tyr694) monoclonal antibody, unconjugated, clone E208	Abcam, ab32364	Rabbit; monoclonal	1:1000	AB_778105
Anti-STAT5	Amino terminus	Stat5 antibody	Cell Signaling Technologies, 9363S	Rabbit; polyclonal	1:1000	AB_10693321
Anti-STAT5	Sheep Stat5 aa. 451-649	Purified mouse anti-Stat5 clone 89/Stat5 (RUO)	BD Biosciences, 610192	Mouse; monoclonal	1:1000	AB_397591
Anti-ATM			Gene Tex (clone 2C1)		1:3000	AB_368161
Anti-phospho-S1981 ATM			Epitomics, clone EP1890Y, Cedarlane	Rabbit; monoclonal	1:5000	AB_991678
Anti-hsp90alpha			StressGen, catalog SPS-771	Rabbit	1:5000	AB_1534201
Jak2 (D2E12) XP rabbit mAb antibody			Cell Signaling Technologies, 3230	Rabbit; monoclonal	1:5000	AB_2128522
Anti–histone H3	KLH-conjugated linear peptide corresponding to the *N*-terminus of human histone H3	Anti–histone H3 antibody	Millipore, 06-755	Rabbit; polyclonal	1:1000	AB_11211742

Abbreviations: ECD, extracellular domain; RRID, Research Resource Identifier.

References

1. Arendt LM, Kuperwasser C. Form and function: how estrogen and progesterone regulate the mammary epithelial hierarchy. *J Mammary Gland Biol Neoplasia*. 2015;**20**(1–2):9–25.
2. Shemanko CS. Prolactin receptor in breast cancer: marker for metastatic risk. *J Mol Endocrinol*. 2016;**57**(4):R153–R165.
3. Shemanko CS, Cong Y, Forsyth A. What is breast in the bone? *Int J Mol Sci*. 2016;**17**(10):1764.
4. Sutherland A, Forsyth A, Cong Y, Grant L, Juan TH, Lee JK, Klimowicz A, Petrillo SK, Hu J, Chan A, Boutillon F, Goffin V, Egan C, Tang PA, Cai L, Morris D, Magliocco A, Shemanko CS. The role of prolactin in bone metastasis and breast cancer cell-mediated osteoclast differentiation. *J Natl Cancer Inst*. 2015; **108**(3):djv338.
5. LaPensee EW, Ben-Jonathan N. Novel roles of prolactin and estrogens in breast cancer: resistance to chemotherapy. *Endocr Relat Cancer*. 2010;**17**(2):R91–R107.
6. Lissoni P, Vaghi M, Ardizzoia A, Fumagalli E, Tancini G, Gardani G, Conti A, Maestroni GJ. Efficacy of monochemotherapy with docetaxel (Taxotere) in relation to prolactin secretion in heavily pretreated metastatic breast cancer. *Neuroendocrinol Lett*. 2001; **22**(1):27–29.
7. Mujagić Z, Mujagić H. Importance of serum prolactin determination in metastatic breast cancer patients. *Croat Med J*. 2004;**45**(2):176–180.
8. Tikk K, Sookthai D, Johnson T, Rinaldi S, Romieu I, Tjønneland A, Olsen A, Overvad K, Clavel-Chapelon F, Baglietto L, Boeing H, Trichopoulou A, Lagiou P, Trichopoulos D, Palli D, Pala V, Tumino R, Rosso S, Panico S, Agudo A, Menéndez V, Sánchez MJ, Amiano P, Huerta Castaño JM, Ardanaz E, Bueno-de-Mesquita HB, Monninkhof E, Onland-Moret C, Andersson A, Sund M, Weiderpass E, Khaw KT, Key TJ, Travis RC, Gunter MJ, Riboli E, Dossus L, Kaaks R. Circulating prolactin and breast cancer risk among pre- and postmenopausal women in the EPIC cohort. *Ann Oncol*. 2014;**25**(7):1422–1428.
9. Tworoger SS, Eliassen AH, Zhang X, Qian J, Sluss PM, Rosner BA, Hankinson SE. A 20-year prospective study of plasma prolactin as a risk marker of breast cancer development. *Cancer Res*. 2013;**73**(15):4810–4819.
10. Rose-Hellekant TA, Arendt LM, Schroeder MD, Gilchrist K, Sandgren EP, Schuler LA. Prolactin induces ERalpha-positive and ERalpha-negative mammary cancer in transgenic mice. *Oncogene*. 2003;**22**(30):4664–4674.
11. Wennbo H, Gebre-Medhin M, Gritli-Linde A, Ohlsson C, Isaksson OG, Törnell J. Activation of the prolactin receptor but

not the growth hormone receptor is important for induction of mammary tumors in transgenic mice. *J Clin Invest*. 1997;**100**(11): 2744–2751.
12. Clevenger CV. Role of prolactin/prolactin receptor signaling in human breast cancer. *Breast Dis*. 2003;**18**(1):75–86.
13. Hachim IY, Hachim MY, Lopez VM, Lebrun JJ, Ali S. Prolactin receptor expression is an independent favorable prognostic marker in human breast cancer. *Appl Immunohistochem Mol Morphol*. 2016;**24**(4):238–245.
14. Hachim IY, Shams A, Lebrun JJ, Ali S. A favorable role of prolactin in human breast cancer reveals novel pathway-based gene signatures indicative of tumor differentiation and favorable patient outcome. *Hum Pathol*. 2016;**53**:142–152.
15. Plotnikov A, Varghese B, Tran TH, Liu C, Rui H, Fuchs SY. Impaired turnover of prolactin receptor contributes to transformation of human breast cells. *Cancer Res*. 2009;**69**(7): 3165–3172.
16. Yonezawa T, Chen KH, Ghosh MK, Rivera L, Dill R, Ma L, Villa PA, Kawaminami M, Walker AM. Anti-metastatic outcome of isoform-specific prolactin receptor targeting in breast cancer. *Cancer Lett*. 2015;**366**(1):84–92.
17. Boutin JM, Edery M, Shirota M, Jolicoeur C, Lesueur L, Ali S, Gould D, Djiane J, Kelly PA. Identification of a cDNA encoding a long form of prolactin receptor in human hepatoma and breast cancer cells. *Mol Endocrinol*. 1989;**3**(9):1455–1461.
18. Kline JB, Roehrs H, Clevenger CV. Functional characterization of the intermediate isoform of the human prolactin receptor. *J Biol Chem*. 1999;**274**(50):35461–35468.
19. Meng J, Tsai-Morris CH, Dufau ML. Human prolactin receptor variants in breast cancer: low ratio of short forms to the long-form human prolactin receptor associated with mammary carcinoma. *Cancer Res*. 2004;**64**(16):5677–5682.
20. Trott JF, Hovey RC, Koduri S, Vonderhaar BK. Alternative splicing to exon 11 of human prolactin receptor gene results in multiple isoforms including a secreted prolactin-binding protein. *J Mol Endocrinol*. 2003;**30**(1):31–47.
21. Ginsburg E, Vonderhaar BK. Prolactin synthesis and secretion by human breast cancer cells. *Cancer Res*. 1995;**55**(12):2591–2595.
22. Abdelmagid SA, Too CK. Prolactin and estrogen up-regulate carboxypeptidase-d to promote nitric oxide production and survival of mcf-7 breast cancer cells. *Endocrinology*. 2008; **149**(10):4821–4828.
23. Chakravarti P, Henry MK, Quelle FW. Prolactin and heregulin override DNA damage-induced growth arrest and promote phosphatidylinositol-3 kinase-dependent proliferation in breast cancer cells. *Int J Oncol*. 2005;**26**(2):509–514.
24. Chen WY, Ramamoorthy P, Chen N, Sticca R, Wagner TE. A human prolactin antagonist, hPRL-G129R, inhibits breast cancer cell proliferation through induction of apoptosis. *Clin Cancer Res*. 1999;**5**(11):3583–3593.
25. Perks CM, Keith AJ, Goodhew KL, Savage PB, Winters ZE, Holly JM. Prolactin acts as a potent survival factor for human breast cancer cell lines. *Br J Cancer*. 2004;**91**(2):305–311.
26. Wu ZS, Yang K, Wan Y, Qian PX, Perry JK, Chiesa J, Mertani HC, Zhu T, Lobie PE. Tumor expression of human growth hormone and human prolactin predict a worse survival outcome in patients with mammary or endometrial carcinoma. *J Clin Endocrinol Metab*. 2011;**96**(10):E1619–E1629.
27. Anderson E, Ferguson JE, Morten H, Shalet SM, Robinson EL, Howell A. Serum immunoreactive and bioactive lactogenic hormones in advanced breast cancer patients treated with bromocriptine and octreotide. *Eur J Cancer*. 1993;**29A**(2): 209–217.
28. Bonneterre J, Mauriac L, Weber B, Roche H, Fargeot P, Tubiana-Hulin M, Sevin M, Chollet P, Cappelaere P. Tamoxifen plus bromocriptine versus tamoxifen plus placebo in advanced breast cancer: results of a double blind multicentre clinical trial. *Eur J Cancer Clin Oncol*. 1988;**24**(12):1851–1853.
29. Clevenger CV, Zheng J, Jablonski EM, Galbaugh TL, Fang F. From bench to bedside: future potential for the translation of prolactin inhibitors as breast cancer therapeutics. *J Mammary Gland Biol Neoplasia*. 2008;**13**(1):147–156.
30. Perotti C, Liu R, Parusel CT, Böcher N, Schultz J, Bork P, Pfitzner E, Groner B, Shemanko CS. Heat shock protein-90-alpha, a prolactin-STAT5 target gene identified in breast cancer cells, is involved in apoptosis regulation. *Breast Cancer Res*. 2008;**10**(6): R94.
31. Swaminathan G, Varghese B, Fuchs SY. Regulation of prolactin receptor levels and activity in breast cancer. *J Mammary Gland Biol Neoplasia*. 2008;**13**(1):81–91.
32. LaPensee EW, Schwemberger SJ, LaPensee CR, Bahassi M, Afton SE, Ben-Jonathan N. Prolactin confers resistance against cisplatin in breast cancer cells by activating glutathione-S-transferase. *Carcinogenesis*. 2009;**30**(8):1298–1304.
33. Howell SJ, Anderson E, Hunter T, Farnie G, Clarke RB. Prolactin receptor antagonism reduces the clonogenic capacity of breast cancer cells and potentiates doxorubicin and paclitaxel cytotoxicity. *Breast Cancer Res*. 2008;**10**(4):R68.
34. Neckers L. Heat shock protein 90: the cancer chaperone. *J Biosci*. 2007;**32**(3):517–530.
35. Workman P, Burrows F, Neckers L, Rosen N. Drugging the cancer chaperone HSP90: combinatorial therapeutic exploitation of oncogene addiction and tumor stress. *Ann N Y Acad Sci*. 2007; **1113**(1):202–216.
36. Pick E, Kluger Y, Giltnane JM, Moeder C, Camp RL, Rimm DL, Kluger HM. High HSP90 expression is associated with decreased survival in breast cancer. *Cancer Res*. 2007;**67**(7):2932–2937.
37. Yano M, Naito Z, Tanaka S, Asano G. Expression and roles of heat shock proteins in human breast cancer. *Jpn J Cancer Res*. 1996;**87**(9):908–915.
38. Yano M, Naito Z, Yokoyama M, Shiraki Y, Ishiwata T, Inokuchi M, Asano G. Expression of hsp90 and cyclin D1 in human breast cancer. *Cancer Lett*. 1999;**137**(1):45–51.
39. Teng SC, Chen YY, Su YN, Chou PC, Chiang YC, Tseng SF, Wu KJ. Direct activation of HSP90A transcription by c-Myc contributes to c-Myc-induced transformation. *J Biol Chem*. 2004; **279**(15):14649–14655.
40. Eustace BK, Sakurai T, Stewart JK, Yimlamai D, Unger C, Zehetmeier C, Lain B, Torella C, Henning SW, Beste G, Scroggins BT, Neckers L, Ilag LL, Jay DG. Functional proteomic screens reveal an essential extracellular role for hsp90 alpha in cancer cell invasiveness. *Nat Cell Biol*. 2004;**6**(6):507–514.
41. Alarcon SV, Mollapour M, Lee MJ, Tsutsumi S, Lee S, Kim YS, Prince T, Apolo AB, Giaccone G, Xu W, Neckers LM, Trepel JB. Tumor-intrinsic and tumor-extrinsic factors impacting hsp90-targeted therapy. *Curr Mol Med*. 2012;**12**(9):1125–1141.
42. Beliakoff J, Whitesell L. Hsp90: an emerging target for breast cancer therapy. *Anticancer Drugs*. 2004;**15**(7):651–662.
43. Modi S, Stopeck AT, Gordon MS, Mendelson D, Solit DB, Bagatell R, Ma W, Wheler J, Rosen N, Norton L, Cropp GF, Johnson RG, Hannah AL, Hudis CA. Combination of trastuzumab and tanespimycin (17-AAG, KOS-953) is safe and active in trastuzumab-refractory HER-2 overexpressing breast cancer: a phase I dose-escalation study. *J Clin Oncol*. 2007;**25**(34): 5410–5417.
44. Sharp S, Workman P. Inhibitors of the HSP90 molecular chaperone: current status. *Adv Cancer Res*. 2006;**95**:323–348.
45. Taipale M, Jarosz DF, Lindquist S. HSP90 at the hub of protein homeostasis: emerging mechanistic insights. *Nat Rev Mol Cell Biol*. 2010;**11**(7):515–528.
46. Trepel J, Mollapour M, Giaccone G, Neckers L. Targeting the dynamic HSP90 complex in cancer. *Nat Rev Cancer*. 2010;**10**(8): 537–549.
47. Lundgren K, Zhang H, Brekken J, Huser N, Powell RE, Timple N, Busch DJ, Neely L, Sensintaffar JL, Yang YC, McKenzie A, Friedman J, Scannevin R, Kamal A, Hong K, Kasibhatla SR,

Boehm MF, Burrows FJ. BIIB021, an orally available, fully synthetic small-molecule inhibitor of the heat shock protein Hsp90. *Mol Cancer Ther*. 2009;**8**(4):921–929.
48. Kamal A, Thao L, Sensintaffar J, Zhang L, Boehm MF, Fritz LC, Burrows FJ. A high-affinity conformation of Hsp90 confers tumour selectivity on Hsp90 inhibitors. *Nature*. 2003;**425**(6956): 407–410.
49. Lee CH, Hong HM, Chang YY, Chang WW. Inhibition of heat shock protein (Hsp) 27 potentiates the suppressive effect of Hsp90 inhibitors in targeting breast cancer stem-like cells. *Biochimie*. 2012;**94**(6):1382–1389.
50. Bareng J, Jilani I, Gorre M, Kantarjian H, Giles F, Hannah A, Albitar M. A potential role for HSP90 inhibitors in the treatment of JAK2 mutant-positive diseases as demonstrated using quantitative flow cytometry. *Leuk Lymphoma*. 2007;**48**(11): 2189–2195.
51. Marubayashi S, Koppikar P, Taldone T, Abdel-Wahab O, West N, Bhagwat N, Caldas-Lopes E, Ross KN, Gönen M, Gozman A, Ahn JH, Rodina A, Ouerfelli O, Yang G, Hedvat C, Bradner JE, Chiosis G, Levine RL. HSP90 is a therapeutic target in JAK2-dependent myeloproliferative neoplasms in mice and humans. *J Clin Invest*. 2010;**120**(10):3578–3593.
52. Fang Q, Inanc B, Schamus S, Wang XH, Wei L, Brown AR, Svilar D, Sugrue KF, Goellner EM, Zeng X, Yates NA, Lan L, Vens C, Sobol RW. HSP90 regulates DNA repair via the interaction between XRCC1 and DNA polymerase β. *Nat Commun*. 2014;**5**: 5513.
53. Stecklein SR, Kumaraswamy E, Behbod F, Wang W, Chaguturu V, Harlan-Williams LM, Jensen RA. BRCA1 and HSP90 cooperate in homologous and non-homologous DNA double-strand-break repair and G2/M checkpoint activation. *Proc Natl Acad Sci USA*. 2012;**109**(34):13650–13655.
54. Arlander SJ, Eapen AK, Vroman BT, McDonald RJ, Toft DO, Karnitz LM. Hsp90 inhibition depletes Chk1 and sensitizes tumor cells to replication stress. *J Biol Chem*. 2003;**278**(52): 52572–52577.
55. Ha K, Fiskus W, Rao R, Balusu R, Venkannagari S, Nalabothula NR, Bhalla KN. Hsp90 inhibitor-mediated disruption of chaperone association of ATR with hsp90 sensitizes cancer cells to DNA damage. *Mol Cancer Ther*. 2011;**10**(7):1194–1206.
56. Dote H, Burgan WE, Camphausen K, Tofilon PJ. Inhibition of hsp90 compromises the DNA damage response to radiation. *Cancer Res*. 2006;**66**(18):9211–9220.
57. Horejsí Z, Takai H, Adelman CA, Collis SJ, Flynn H, Maslen S, Skehel JM, de Lange T, Boulton SJ. CK2 phospho-dependent binding of R2TP complex to TEL2 is essential for mTOR and SMG1 stability. *Mol Cell*. 2010;**39**(6):839–850.
58. Takai H, Xie Y, de Lange T, Pavletich NP. Tel2 structure and function in the Hsp90-dependent maturation of mTOR and ATR complexes. *Genes Dev*. 2010;**24**(18):2019–2030.
59. Takai H, Wang RC, Takai KK, Yang H, de Lange T. Tel2 regulates the stability of PI3K-related protein kinases. *Cell*. 2007;**131**(7): 1248–1259.
60. Hurov KE, Cotta-Ramusino C, Elledge SJ. A genetic screen identifies the Triple T complex required for DNA damage signaling and ATM and ATR stability. *Genes Dev*. 2010;**24**(17): 1939–1950.
61. Blackford AN, Jackson SP. ATM, ATR, and DNA-PK: the trinity at the heart of the DNA damage response. *Mol Cell*. 2017;**66**(6): 801–817.
62. Goodarzi AA, Jeggo P, Lobrich M. The influence of heterochromatin on DNA double strand break repair: Getting the strong, silent type to relax. *DNA Repair (Amst)*. 2010;**9**(12): 1273–1282.
63. Goodarzi AA, Kurka T, Jeggo PA. KAP-1 phosphorylation regulates CHD3 nucleosome remodeling during the DNA double-strand break response. *Nat Struct Mol Biol*. 2011;**18**(7): 831–839.
64. Álvarez-Quilón A, Serrano-Benítez A, Lieberman JA, Quintero C, Sánchez-Gutiérrez D, Escudero LM, Cortés-Ledesma F. ATM specifically mediates repair of double-strand breaks with blocked DNA ends. *Nat Commun*. 2014;**5**:3347.
65. Vologodskii A. Disentangling DNA molecules. *Phys Life Rev*. 2016;**18**:118–134.
66. Bernichtein S, Kayser C, Dillner K, Moulin S, Kopchick JJ, Martial JA, Norstedt G, Isaksson O, Kelly PA, Goffin V. Development of pure prolactin receptor antagonists. *J Biol Chem*. 2003;**278**(38): 35988–35999.
67. Perotti C, Wiedl T, Florin L, Reuter H, Moffat S, Silbermann M, Hahn M, Angel P, Shemanko CS. Characterization of mammary epithelial cell line HC11 using the NIA 15k gene array reveals potential regulators of the undifferentiated and differentiated phenotypes. *Differentiation*. 2009;**78**(5):269–282.
68. Schneider CA, Rasband WS, Eliceiri KW. NIH Image to ImageJ: 25 years of image analysis. *Nat Methods*. 2012;**9**(7):671–675.
69. Berkovich E, Monnat RJ, Jr, Kastan MB. Roles of ATM and NBS1 in chromatin structure modulation and DNA double-strand break repair. *Nat Cell Biol*. 2007;**9**(6):683–690.
70. Chou TC. Theoretical basis, experimental design, and computerized simulation of synergism and antagonism in drug combination studies. *Pharmacol Rev*. 2006;**58**(3):621–681.
71. Salerno S, Da Settimo F, Taliani S, Simorini F, La Motta C, Fornaciari G, Marini AM. Recent advances in the development of dual topoisomerase I and II inhibitors as anticancer drugs. *Curr Med Chem*. 2010;**17**(35):4270–4290.
72. Kurz EU, Lees-Miller SP. DNA damage-induced activation of ATM and ATM-dependent signaling pathways. *DNA Repair (Amst)*. 2004;**3**(8-9):889–900.
73. Muslimović A, Nyström S, Gao Y, Hammarsten O. Numerical analysis of etoposide induced DNA breaks [published correction appears in *PLoS ONE*. 4(6):10.1371/annotation/290cebfd-d5dc-4bd2-99b4-f4cf0be6c838]. *PLoS One*. 2009;**4**(6):e5859.
74. Bakkenist CJ, Kastan MB. DNA damage activates ATM through intermolecular autophosphorylation and dimer dissociation. *Nature*. 2003;**421**(6922):499–506.
75. Brandes AH, Ward CS, Ronen SM. 17-allyamino-17-demethoxygeldanamycin treatment results in a magnetic resonance spectroscopy-detectable elevation in choline-containing metabolites associated with increased expression of choline transporter SLC44A1 and phospholipase A2. *Breast Cancer Res*. 2010;**12**(5):R84.
76. Utama FE, Tran TH, Ryder A, LeBaron MJ, Parlow AF, Rui H. Insensitivity of human prolactin receptors to nonhuman prolactins: relevance for experimental modeling of prolactin receptor-expressing human cells. *Endocrinology*. 2009;**150**(4):1782–1790.
77. Tworoger SS, Eliassen AH, Rosner B, Sluss P, Hankinson SE. Plasma prolactin concentrations and risk of postmenopausal breast cancer. *Cancer Res*. 2004;**64**(18):6814–6819.
78. Tworoger SS, Eliassen AH, Sluss P, Hankinson SE. A prospective study of plasma prolactin concentrations and risk of premenopausal and postmenopausal breast cancer. *J Clin Oncol*. 2007;**25**(12):1482–1488.
79. Tworoger SS, Hankinson SE. Prolactin and breast cancer etiology: an epidemiologic perspective. *J Mammary Gland Biol Neoplasia*. 2008;**13**(1):41–53.
80. Urbanska A. *Prolactin-Mediated Breast Cancer Cell Resistance to DNA Damaging Agents Involves HSP90*. Calgary, Canada: Biological Sciences, University of Calgary; 2011.
81. Wakao H, Gouilleux F, Groner B. Mammary gland factor (MGF) is a novel member of the cytokine regulated transcription factor gene family and confers the prolactin response. *EMBO J*. 1994; **13**(9):2182–2191.
82. Karayazi Atici Ö. *The Role of Prolactin in the Cellular Response to DNA Damaging Agents*. Calgary, Canada: Biological Sciences, University of Calgary; 2015.

83. Kiss R, Polgár T, Kirabo A, Sayyah J, Figueroa NC, List AF, Sokol L, Zuckerman KS, Gali M, Bisht KS, Sayeski PP, Keseru GM. Identification of a novel inhibitor of JAK2 tyrosine kinase by structure-based virtual screening. *Bioorg Med Chem Lett*. 2009; **19**(13):3598–3601.
84. Rainey MD, Charlton ME, Stanton RV, Kastan MB. Transient inhibition of ATM kinase is sufficient to enhance cellular sensitivity to ionizing radiation. *Cancer Res*. 2008;**68**(18):7466–7474.
85. Camphausen K, Tofilon PJ. Inhibition of Hsp90: a multitarget approach to radiosensitization. *Clin Cancer Res*. 2007;**13**(15 Pt 1):4326–4330.
86. Matsumoto Y, Machida H, Kubota N. Preferential sensitization of tumor cells to radiation by heat shock protein 90 inhibitor geldanamycin. *J Radiat Res (Tokyo)*. 2005;**46**(2):215–221.
87. Münster PN, Basso A, Solit D, Norton L, Rosen N. Modulation of Hsp90 function by ansamycins sensitizes breast cancer cells to chemotherapy-induced apoptosis in an RB- and schedule-dependent manner. See: E. A. Sausville, Combining cytotoxics and 17-allylamino, 17-demethoxygeldanamycin: sequence and tumor biology matters, Clin. Cancer Res., 7: 2155–2158, 2001. *Clin Cancer Res*. 2001;**7**(8):2228–2236.
88. Tillotson B, Slocum K, Coco J, Whitebread N, Thomas B, West KA, MacDougall J, Ge J, Ali JA, Palombella VJ, Normant E, Adams J, Fritz CC. Hsp90 (heat shock protein 90) inhibitor occupancy is a direct determinant of client protein degradation and tumor growth arrest in vivo. *J Biol Chem*. 2010;**285**(51): 39835–39843.
89. Powers MV, Valenti M, Miranda S, Maloney A, Eccles SA, Thomas G, Clarke PA, Workman P. Mode of cell death induced by the HSP90 inhibitor 17-AAG (tanespimycin) is dependent on the expression of pro-apoptotic BAX. *Oncotarget*. 2013;**4**(11):1963–1975.
90. Kagawa S, Gu J, Honda T, McDonnell TJ, Swisher SG, Roth JA, Fang B. Deficiency of caspase-3 in MCF7 cells blocks Bax-mediated nuclear fragmentation but not cell death. *Clin Cancer Res*. 2001;**7**(5):1474–1480.
91. Thompson C, MacDonald G, Mueller CR. Decreased expression of BRCA1 in SK-BR-3 cells is the result of aberrant activation of the GABP Beta promoter by an NRF-1-containing complex. *Mol Cancer*. 2011;**10**(1):62.
92. Radhakrishnan A, Raju R, Tuladhar N, Subbannayya T, Thomas JK, Goel R, Telikicherla D, Palapetta SM, Rahiman BA, Venkatesh DD, Urmila KK, Harsha HC, Mathur PP, Prasad TS, Pandey A, Shemanko C, Chatterjee A. A pathway map of prolactin signaling. *J Cell Commun Signal*. 2012;**6**(3):169–173.
93. Waters MJ, Brooks AJ. JAK2 activation by growth hormone and other cytokines. *Biochem J*. 2015;**466**(1):1–11.
94. Domanska D, Brzezianska E. Review: the JAK/STAT protein activation—role in cancer development and targeted therapy. *Curr Signal Transduct Ther*. 2012;**7**(3):187–201.
95. Rädler PD, Wehde BL, Wagner KU. Crosstalk between STAT5 activation and PI3K/AKT functions in normal and transformed mammary epithelial cells. *Mol Cell Endocrinol*. 2017;**451**(C):31–39.
96. Sakamoto K, Triplett AA, Schuler LA, Wagner KU. Janus kinase 2 is required for the initiation but not maintenance of prolactin-induced mammary cancer. *Oncogene*. 2010;**29**(39):5359–5369.
97. Wagner KU, Schmidt JW. The two faces of Janus kinases and their respective STATs in mammary gland development and cancer. *J Carcinog*. 2011;**10**(1):32.
98. Aznar S, Valerón PF, del Rincon SV, Pérez LF, Perona R, Lacal JC. Simultaneous tyrosine and serine phosphorylation of STAT3 transcription factor is involved in Rho A GTPase oncogenic transformation. *Mol Biol Cell*. 2001;**12**(10):3282–3294.
99. Cataldo L, Chen NY, Yuan Q, Li W, Ramamoorthy P, Wagner TE, Sticca RP, Chen WY. Inhibition of oncogene STAT3 phosphorylation by a prolactin antagonist, hPRL-G129R, in T-47D human breast cancer cells. *Int J Oncol*. 2000;**17**(6):1179–1185.
100. Neilson LM, Zhu J, Xie J, Malabarba MG, Sakamoto K, Wagner KU, Kirken RA, Rui H. Coactivation of Janus tyrosine kinase (Jak)1 positively modulates prolactin-Jak2 signaling in breast cancer: recruitment of ERK and signal transducer and activator of transcription (Stat)3 and enhancement of Akt and Stat5a/b pathways. *Mol Endocrinol*. 2007;**21**(9):2218–2232.
101. Clevenger CV. Roles and regulation of Stat family transcription factors in human breast cancer. *Am J Pathol*. 2004;**165**(5): 1449–1460.
102. Berishaj M, Gao SP, Ahmed S, Leslie K, Al-Ahmadie H, Gerald WL, Bornmann W, Bromberg JF. Stat3 is tyrosine-phosphorylated through the interleukin-6/glycoprotein 130/Janus kinase pathway in breast cancer. *Breast Cancer Res*. 2007;**9**(3):R32.
103. Burke WM, Jin X, Lin HJ, Huang M, Liu R, Reynolds RK, Lin J. Inhibition of constitutively active Stat3 suppresses growth of human ovarian and breast cancer cells. *Oncogene*. 2001;**20**(55): 7925–7934.
104. Barbieri I, Pensa S, Pannellini T, Quaglino E, Maritano D, Demaria M, Voster A, Turkson J, Cavallo F, Watson CJ, Provero P, Musiani P, Poli V. Constitutively active Stat3 enhances neu-mediated migration and metastasis in mammary tumors via upregulation of Cten. *Cancer Res*. 2010;**70**(6):2558–2567.
105. Marotta LL, Almendro V, Marusyk A, Shipitsin M, Schemme J, Walker SR, Bloushtain-Qimron N, Kim JJ, Choudhury SA, Maruyama R, Wu Z, Gönen M, Mulvey LA, Bessarabova MO, Huh SJ, Silver SJ, Kim SY, Park SY, Lee HE, Anderson KS, Richardson AL, Nikolskaya T, Nikolsky Y, Liu XS, Root DE, Hahn WC, Frank DA, Polyak K. The JAK2/STAT3 signaling pathway is required for growth of $CD44^{+}CD24^{-}$ stem cell–like breast cancer cells in human tumors. *J Clin Invest*. 2011;**121**(7):2723–2735.
106. Goffin V. Prolactin receptor targeting in breast and prostate cancers: new insights into an old challenge. *Pharmacol Ther*. 2017;**179**:111–126.
107. Hong S, Laimins LA. The JAK-STAT transcriptional regulator, STAT-5, activates the ATM DNA damage pathway to induce HPV 31 genome amplification upon epithelial differentiation. *PLoS Pathog*. 2013;**9**(4):e1003295.
108. Mayama J, Kumano T, Hayakari M, Yamazaki T, Aizawa S, Kudo T, Tsuchida S. Polymorphic glutathione S-transferase subunit 3 of rat liver exhibits different susceptibilities to carbon tetrachloride: differences in their interactions with heat-shock protein 90. *Biochem J*. 2003;**372**(Pt 2):611–616.
109. Brisken C. Hormonal control of alveolar development and its implications for breast carcinogenesis. *J Mammary Gland Biol Neoplasia*. 2002;**7**(1):39–48.
110. Bertucci F, Nasser V, Granjeaud S, Eisinger F, Adelaïde J, Tagett R, Loriod B, Giaconia A, Benziane A, Devilard E, Jacquemier J, Viens P, Nguyen C, Birnbaum D, Houlgatte R. Gene expression profiles of poor-prognosis primary breast cancer correlate with survival. *Hum Mol Genet*. 2002;**11**(8):863–872.
111. Powers MV, Workman P. Targeting of multiple signalling pathways by heat shock protein 90 molecular chaperone inhibitors. *Endocr Relat Cancer*. 2006;**13**(suppl 1):S125–S135.
112. Aligue R, Akhavan-Niak H, Russell P. A role for Hsp90 in cell cycle control: Wee1 tyrosine kinase activity requires interaction with Hsp90. *EMBO J*. 1994;**13**(24):6099–6106.
113. Ko JC, Chen HJ, Huang YC, Tseng SC, Weng SH, Wo TY, Huang YJ, Chiu HC, Tsai MS, Chiou RY, Lin YW. HSP90 inhibition induces cytotoxicity via down-regulation of Rad51 expression and DNA repair capacity in non-small cell lung cancer cells. *Regul Toxicol Pharmacol*. 2012;**64**(3):415–424.
114. Barker CR, Hamlett J, Pennington SR, Burrows F, Lundgren K, Lough R, Watson AJ, Jenkins JR. The topoisomerase II-Hsp90 complex: a new chemotherapeutic target? *Int J Cancer*. 2006; **118**(11):2685–2693.
115. Russell JS, Burgan W, Oswald KA, Camphausen K, Tofilon PJ. Enhanced cell killing induced by the combination of radiation and the heat shock protein 90 inhibitor 17-allylamino-17-demethoxygeldanamycin: a multitarget approach to radiosensitization. *Clin Cancer Res*. 2003;**9**(10 Pt 1):3749–3755.

116. Yin X, Zhang H, Lundgren K, Wilson L, Burrows F, Shores CG. BIIB021, a novel Hsp90 inhibitor, sensitizes head and neck squamous cell carcinoma to radiotherapy. *Int J Cancer*. 2010; **126**(5):1216–1225.
117. Hirakawa H, Fujisawa H, Masaoka A, Noguchi M, Hirayama R, Takahashi M, Fujimori A, Okayasu R. The combination of Hsp90 inhibitor 17AAG and heavy-ion irradiation provides effective tumor control in human lung cancer cells. *Cancer Med*. 2015;**4**(3): 426–436.
118. Quanz M, Herbette A, Sayarath M, de Koning L, Dubois T, Sun JS, Dutreix M. Heat shock protein 90α (Hsp90α) is phosphorylated in response to DNA damage and accumulates in repair foci. *J Biol Chem*. 2012;**287**(12):8803–8815.
119. Elaimy AL, Ahsan A, Marsh K, Pratt WB, Ray D, Lawrence TS, Nyati MK. ATM is the primary kinase responsible for phosphorylation of Hsp90α after ionizing radiation. *Oncotarget*. 2016;**7**(50):82450–82457.
120. Guo L, Liu X, Jiang Y, Nishikawa K, Plunkett W. DNA-dependent protein kinase and ataxia telangiectasia mutated (ATM) promote cell survival in response to NK314, a topoisomerase IIα inhibitor. *Mol Pharmacol*. 2011;**80**(2):321–327.
121. Capranico G, De Isabella P, Penco S, Tinelli S, Zunino F. Role of DNA breakage in cytotoxicity of doxorubicin, 9-deoxydoxorubicin, and 4-demethyl-6-deoxydoxorubicin in murine leukemia P388 cells. *Cancer Res*. 1989;**49**(8):2022–2027.
122. Hickson I, Zhao Y, Richardson CJ, Green SJ, Martin NM, Orr AI, Reaper PM, Jackson SP, Curtin NJ, Smith GC. Identification and characterization of a novel and specific inhibitor of the ataxia–telangiectasia mutated kinase ATM. *Cancer Res*. 2004;**64**(24): 9152–9159.